



Original article

Synthesis and *in vitro* antitumor activity of new series of benzothiazole and pyrimido[2,1-*b*]benzothiazole derivatives

Moustafa T. Gabr, Nadia S. El-Gohary*, Eman R. El-Bendary, Mohamed M. El-Kerdawy

Department of Medicinal Chemistry, Faculty of Pharmacy, Mansoura University, Mansoura 35516, Egypt

ARTICLE INFO

Article history:

Received 10 June 2014

Received in revised form

24 July 2014

Accepted 25 July 2014

Available online 29 July 2014

Keywords:

Benzothiazoles

Pyrimidobenzothiazoles

Synthesis

Antitumor activity

Pharmacophore study

ABSTRACT

New series of benzothiazole and pyrimido[2,1-*b*]benzothiazole derivatives were synthesized and characterized by analytical and spectrometrical methods (IR, HRMS, ^1H and ^{13}C NMR). Nineteen of the synthesized compounds were selected by the National Cancer Institute (NCI), USA, to be screened for their antitumor activity at a single dose (10 μM) against a panel of 60 cancer cell lines. The most active compounds, **4**, **6**, **10**, **14**, **17** and **20** were selected for further evaluation at five dose level screening. Compounds **17** (GI_{50} = 0.44 μM , TGI = 1.2 μM and LC_{50} MG-MID = 6.6 μM) and **4** (GI_{50} = 0.77 μM , TGI = 2.08 μM and LC_{50} MG-MID = 11.74 μM) were proved to be the most active members in this study. 3D and 2D pharmacophoric maps for the structural features of both compounds were studied.

© 2014 Elsevier Masson SAS. All rights reserved.

1. Introduction

Cancer is the second most common cause of death after heart disease [1]. During the past decades, cancer continued to be a worldwide killer [2]. Despite the extensive research and rapid progress in cancer treatment, there is a growing demand for new therapies. It is important to identify new agents and new targets for the treatment of cancer. Receptor protein tyrosine kinases play an important role in signal transduction pathways that regulate cell division and differentiation. Epidermal growth factor receptor tyrosine kinase (EGFR-TK) (also known as ErbB-1 or HER-1) and the related human epidermal growth factor receptor (also known as ErbB-2 or HER-2) are among the growth factor receptor kinases that have been identified as being important in cancer [3]. EGFR dependent aberrant signaling is associated with cancer cell proliferation, apoptosis, angiogenesis and metastasis [4]. A number of small molecule EGFR kinase inhibitors have been evaluated in cancer clinical trials. Anilinoquinazoline-containing compounds, erlotinib (Tarceva[®]) [4,5] and gefitinib (Iressa[®]) [6] have been approved for the chemotherapeutic treatment of patients with advanced non-small cell lung cancer. They contain 4-(substituted amino)pyrimidine pharmacophoric core that binds to the hinge

region of the kinase enzyme. Benzothiazole derivatives constitute an important class of therapeutic agents in medicinal chemistry. Literature survey revealed that this nucleus is associated with diverse pharmacological effects, including antitumor [7–18] and antioxidant [19,20] activities. Moreover, pyrimido[2,1-*b*]benzothiazole derivatives have been extensively investigated for their pharmacological uses [7,21–26], some of these compounds showed antitumor activity [7,24–26]. In addition, pyrazole-containing compounds have received considerable attention owing to their diverse chemotherapeutic potentials, including antitumor activity [27–35]. These compounds are able to inhibit different kinds of kinases with powerful antitumor activity [36–38]. On the same line, [1,3,4] oxadiazole-containing compounds exhibited antitumor activity [39–42]. Taking all the above findings into consideration and in searching for new compounds endowed with potent antitumor activity, we report herein the synthesis of new series of benzothiazole and pyrimido[2,1-*b*]benzothiazole derivatives and evaluation of their antitumor activity.

2. Rational and design

Quinazolines have emerged as a versatile template for inhibition of a diverse range of receptor tyrosine kinases. The most widely studied of these receptors is the epidermal growth factor receptor (EGFR); with the small-molecule inhibitor, gefitinib being the first agent from this class to be approved for the treatment of non-small cell lung cancer as EGFR-TK inhibitor [43,44]. Subsequent research

* Corresponding author.

E-mail addresses: dr.nadiaelgohary@yahoo.com, nadiaelgohary2005@gmail.com (N.S. El-Gohary).

aimed at further exploration of the SAR of this novel template led to the discovery of highly selective compounds that target EGFR. Later on, a variety of compounds of structurally diverse chemical classes was proved to be highly potent and selective ATP-competitive inhibitors. Benzothiazoles act *via* competing with ATP for binding at the catalytic domain of EGFR-TK [45]. The ATP-binding site (Fig. 1) has the following features; Adenine region which contains two key hydrogen bonds formed by the interaction of N¹ and N⁶ of the adenine ring. Many potent inhibitors use one of these hydrogen bonds. Sugar pocket which is a hydrophilic region. Hydrophobic regions and channels, though not used by ATP but plays an important role in inhibitor selectivity and binding affinity. Phosphate binding region which is largely solvent exposed and can be used for improving inhibitor selectivity [46].

Our strategy is directed toward designing a variety of ligands which are structurally similar to the basic skeleton, 4-anilinoquinazoline of tinibs (erlotinib and gefitinib) with diverse chemical properties (Fig. 2). Accordingly, we replaced quinazoline ring with benzothiazole since both rings are isosteric with the adenine portion of ATP and can mimic the ATP competitive binding regions of EGFR-TK. The manipulation strategy embraces the incorporation of pyrazole and other azole moieties into the benzothiazole and pyrimido[2,1-*b*]benzothiazole ring systems in order to verify the importance of these moieties for the antitumor activity (Fig. 3).

In our previous work [47,48], compounds **4**, **6**, **10**, **14**, **17** and **20** (with considerable activity against individual cell lines that over-express EGFR) were further evaluated for their EGFR-TK inhibitory activity at Reaction Biology Corporation, USA. Compound **4** displayed the highest EGFR-TK inhibitory activity at the single dose screening; subsequently, it was tested using ten dose IC₅₀ mode and it exhibited IC₅₀ value of 0.239 μM [48]. Compound **4** was also examined over other 10 different human kinases to study its selectivity against EGFR-TK [48].

3. Results and discussion

3.1. Chemistry

A general approach to synthesize the designed compounds is outlined in Schemes 1–5. In Scheme 1, the starting compound, 2-

amino-6-chlorobenzothiazole (**1**) was allowed to react with chloroacetyl chloride in carbon tetrachloride in the presence of triethylamine to produce the chloroacetamide derivative **2** [7]. Reaction of **2** with hydrazine hydrate in ethanol gave the hydrazinylacetamide analog **3** [7].

Concerning Scheme 2, condensation of **3** with diethyl ethoxymethylenemalonate in acetonitrile in the presence of anhydrous potassium carbonate gave the targeted ethyl pyrazole-4-carboxylate derivative **4**. ¹H NMR spectrum of this compound showed the triplet-quartet pattern characteristic for the ethyl protons at δ 1.30 and 4.05–4.35 ppm, respectively. In addition, ¹³C NMR spectrum displayed two signals at δ 14.6 and 61.0 ppm corresponding to ethyl carbons. Reacting **3** with ethyl ethoxymethylenecyanoacetate, ethoxymethylenemalononitrile or ethyl acetoacetate in ethanol in the presence of anhydrous potassium carbonate gave the ethyl pyrazole-4-carboxylate **5**, pyrazole-4-carbonitrile **6** or 4,5-dihydropyrazol-5-one **7**, respectively. The structure of compound **5** was confirmed by the presence of the triplet-quartet pattern characteristic for the ethyl protons at δ 1.30 and 4.28–4.35 ppm, respectively. The structural assignments of compound **6** were based on analytical and spectral data. For example, IR spectrum showed a characteristic absorption band at 2215 cm⁻¹ corresponding to (C≡N) group. The presence of the (C≡N) was further confirmed by the presence of a signal at δ 117.1 ppm in the ¹³C NMR spectrum.

Analogously, compound **8** was synthesized by direct fusion of **3** with diethyl malonate. The IR spectrum of this compound showed three significant absorption bands at 1720, 1686 and 1654 cm⁻¹ corresponding to three (C=O) groups.

When compound **3** was allowed to react with acetylacetone or benzoylacetone in glacial acetic acid, 3,5-dimethyl-1*H*-pyrazole **9** or 3-methyl-5-phenyl-1*H*-pyrazole **10** was obtained, respectively. ¹H NMR spectrum of **9** showed two singlets at δ 2.05 and 2.25 ppm corresponding to two (CH₃) groups. Moreover, ¹³C NMR spectrum of the same compound revealed two signals at δ 20.7 and 23.2 ppm corresponding to two (CH₃) carbons. ¹H NMR spectrum of **10** showed a characteristic singlet at δ 1.90 ppm corresponding to (CH₃) group. In addition, HRMS of the same compound displayed a significant peak at *m/z* [M-H]⁻ 381.0661 which is in agreement with its molecular formula C₁₉H₁₄ClN₄OS⁻.

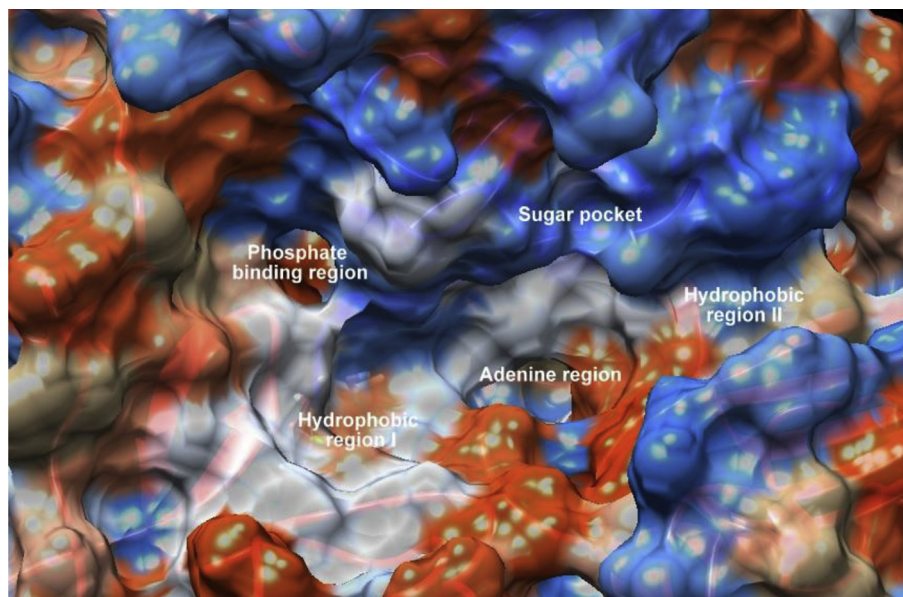


Fig. 1. The molecular surface representation of the ATP-binding site which consists of adenine region, sugar pocket, hydrophobic regions I and II and phosphate binding region [46].

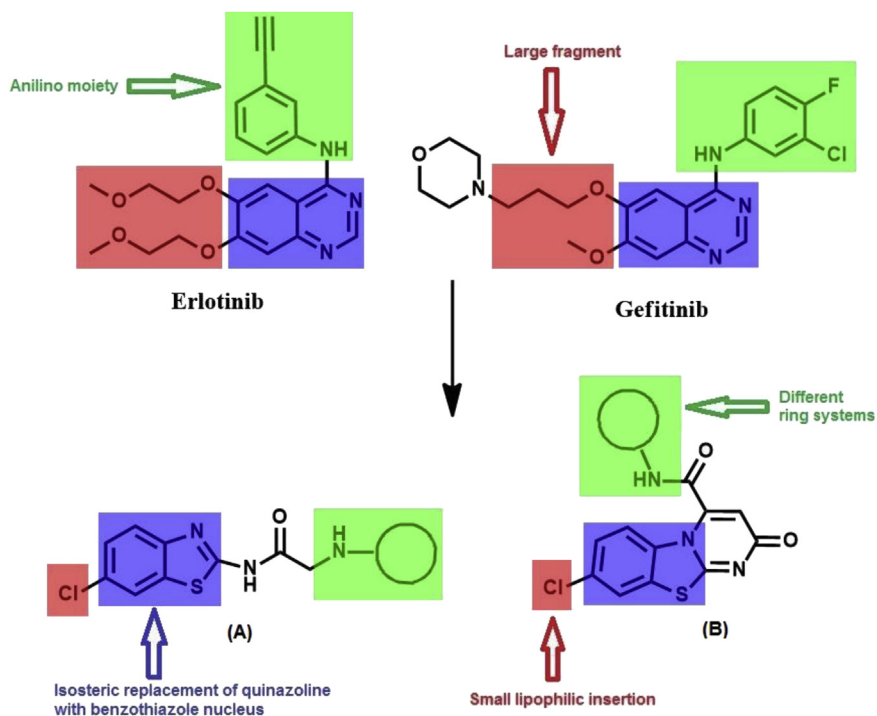


Fig. 2. Reported antitumor quinazolines and proposed analogues incorporating different aryl and heterocyclic moieties; (A) benzothiazole derivatives, (B) pyrimido[2,1-*b*]benzothiazole derivatives.

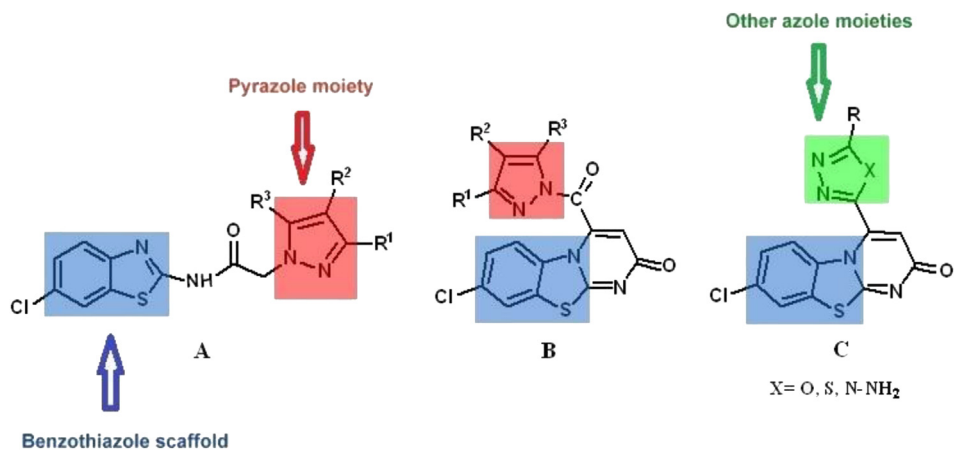
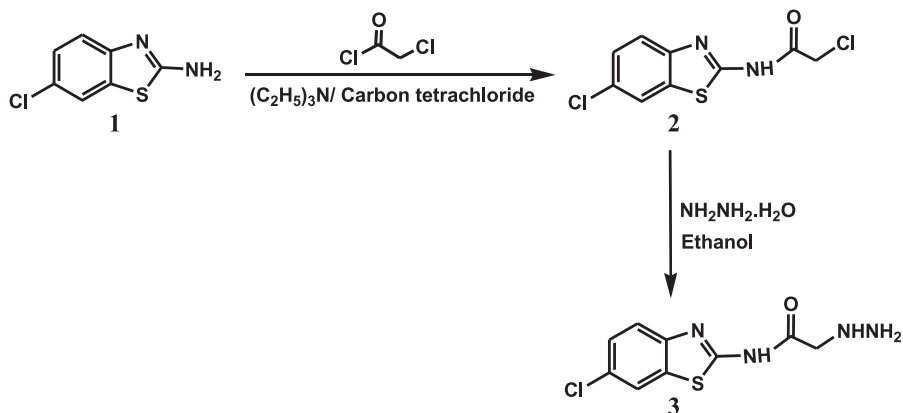
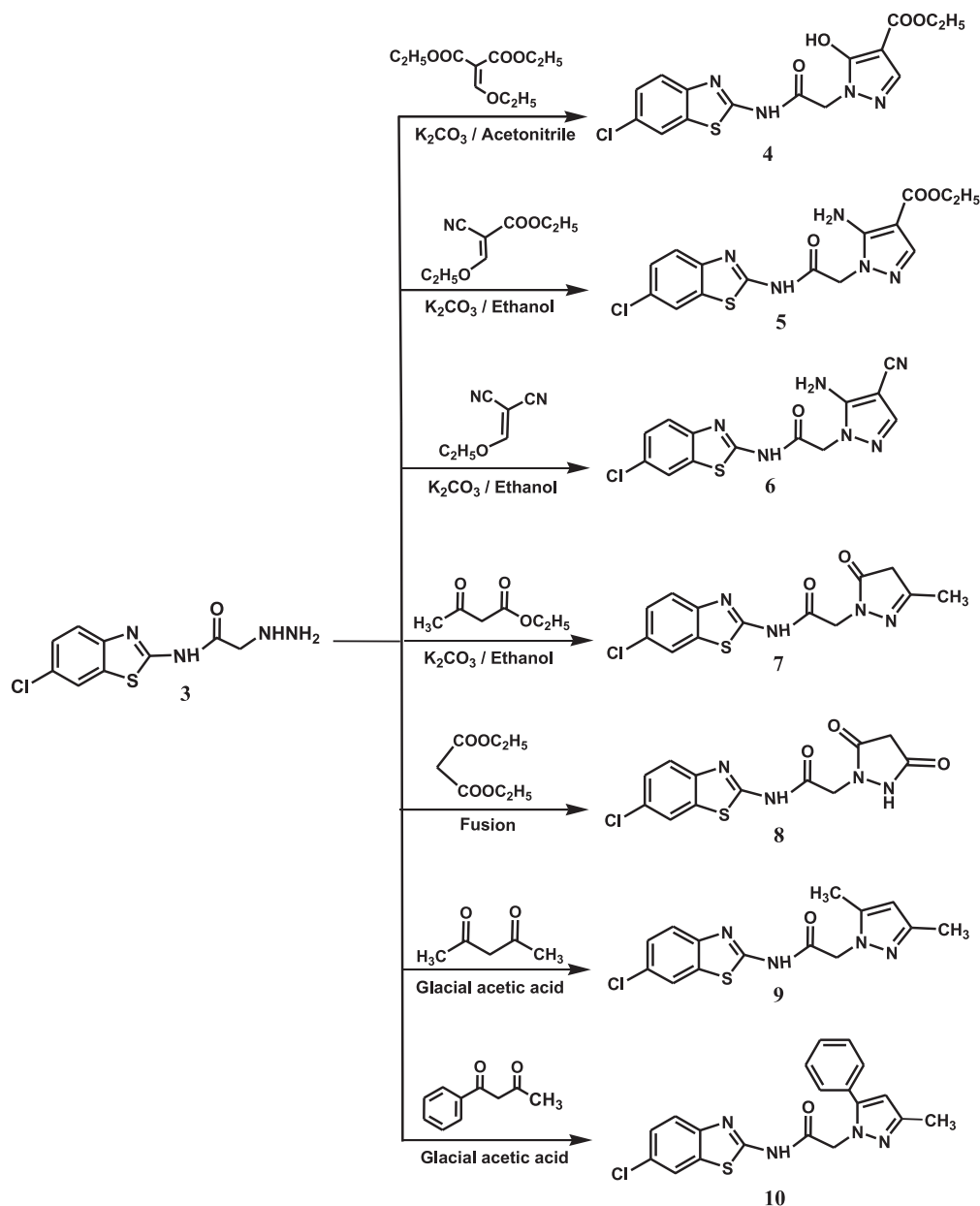


Fig. 3. Incorporation of pyrazole and other azole moieties into the benzothiazole and pyrimido[2,1-*b*]benzothiazole ring systems.



Scheme 1. Synthesis of compound 3.



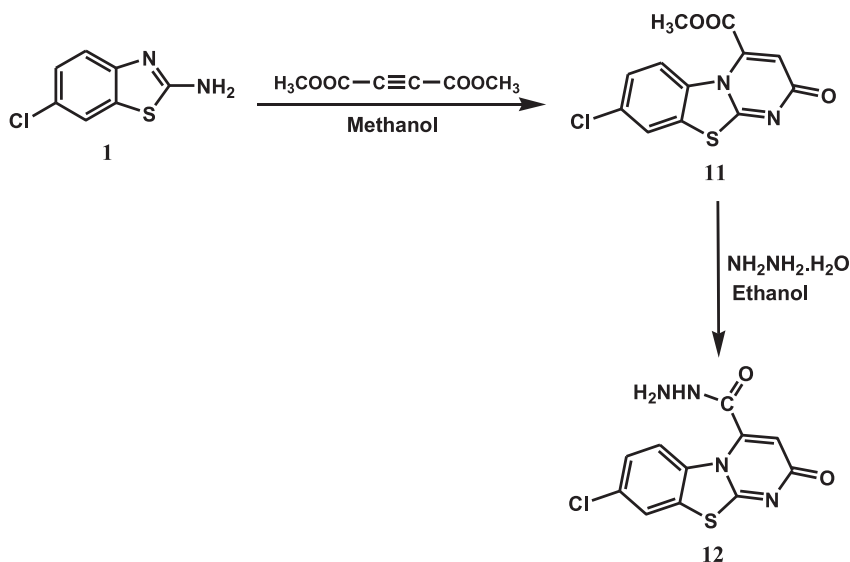
Scheme 2. Synthesis of compounds 4–10.

Concerning Scheme 3, reaction of 2-amino-6-chlorobenzothiazole (1) with dimethyl acetylenedicarboxylate in refluxing methanol gave the targeted methyl pyrimido[2,1-*b*]benzothiazole-4-carboxylate derivative 11 [7]. Reaction of 11 with hydrazine hydrate in ethanol produced the corresponding hydrazide 12 [7].

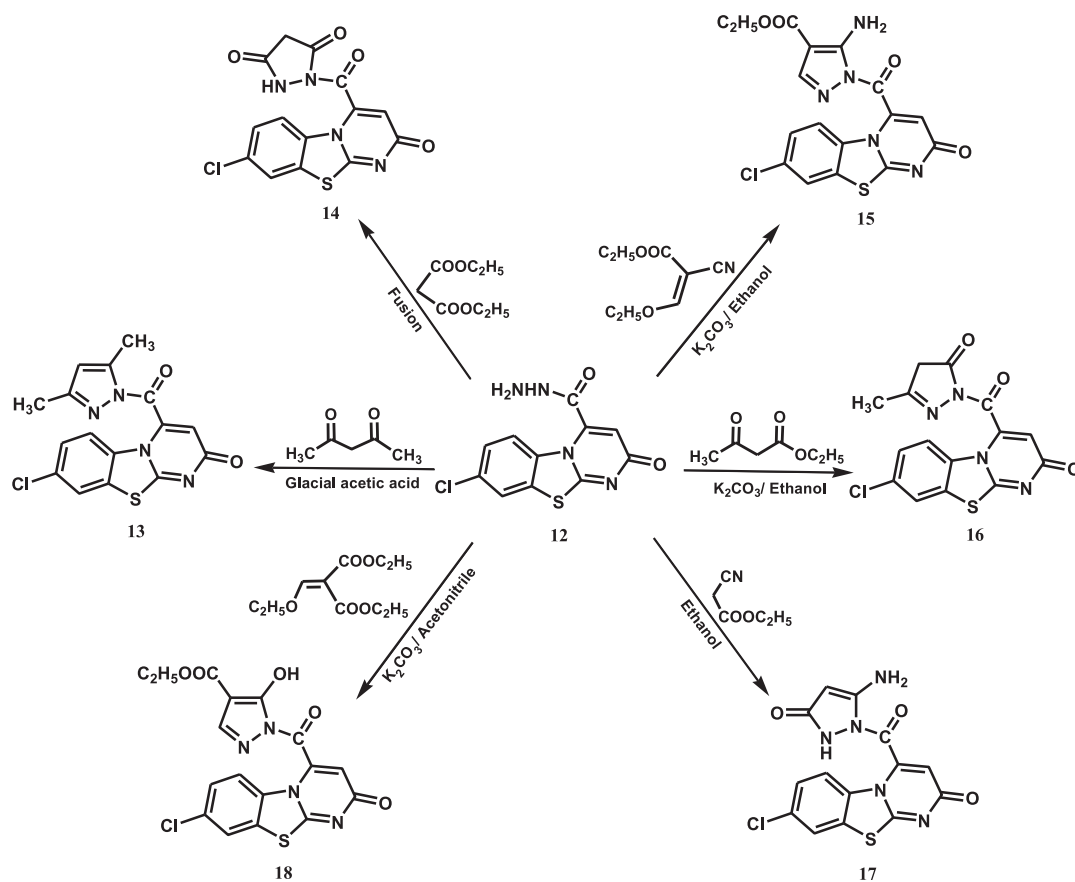
Referring to Scheme 4, condensing 12 with acetylacetone in glacial acetic acid afforded 3,5-dimethyl-1*H*-pyrazole derivative 13. ¹H NMR spectrum of this compound showed two characteristic singlets at δ 2.42 and 2.95 ppm corresponding to two (CH₃) groups. In addition, ¹³C NMR spectrum showed two signals at δ 19.4 and 20.2 ppm corresponding to the two (CH₃) carbons. Heating 12 with diethyl malonate at 200 °C yielded the pyrazolidine-3,5-dione derivative 14. ¹H NMR spectrum of this compound showed a characteristic singlet at δ 4.15 ppm corresponding to (pyrazolidine-H). Furthermore, ¹³C NMR spectrum showed a signal at δ 51.6 ppm corresponding to the (pyrazolidine C-4). Condensing compound 12

with ethyl ethoxymethylenecyanoacetate or ethyl acetoacetate in ethanol in the presence of anhydrous potassium carbonate resulted in the formation of ethyl pyrazole-4-carboxylate 15 or 4,5-dihydropyrazol-5-one 16, respectively. ¹H NMR spectrum of compound 15 showed the triplet-quartet pattern characteristic for the ethyl protons at δ 1.23 and 4.08–4.25 ppm, respectively. ¹H NMR spectrum of 16 showed two characteristic singlets at δ 2.15 and 3.73 ppm corresponding to (CH₃) group and (pyrazoline-H), respectively. Moreover, ¹³C NMR spectrum of the same compound revealed two signals at δ 20.2 and 60.3 ppm corresponding to (CH₃) carbon and (pyrazoline C₄), respectively.

Reacting 12 with ethyl cyanoacetate in ethanol produced 2,3-dihydropyrazol-3-one derivative 17. Reaction of hydrazide 12 with diethyl ethoxymethylenemalonate in acetonitrile in the presence of anhydrous potassium carbonate produced ethyl 5-hydroxy-1*H*-pyrazole-4-carboxylate analog 18. IR spectrum of this compound showed two characteristic absorption bands at 3377



Scheme 3. Synthesis of compound 12.

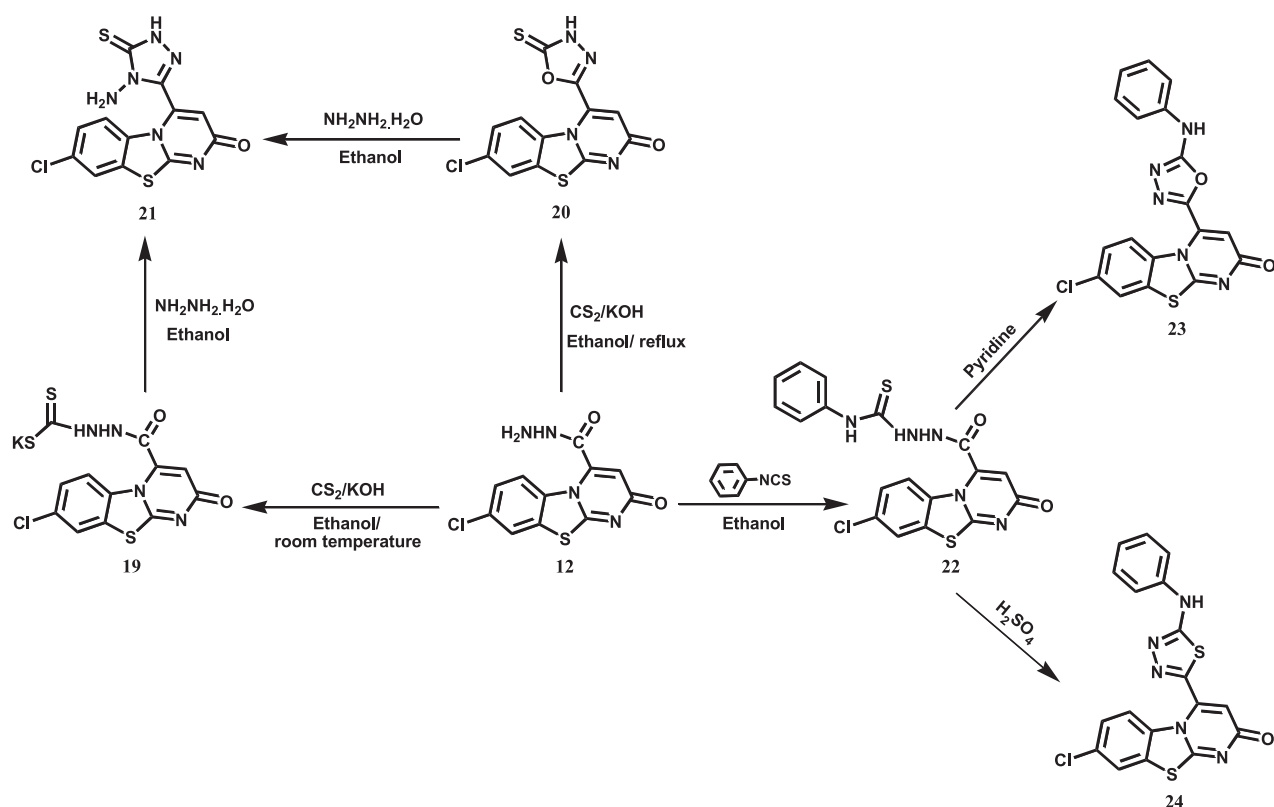


Scheme 4. Synthesis of compounds 13–18.

and 1715 cm^{-1} for (OH) and (COOC_2H_5) groups, respectively. Moreover, ^1H NMR spectrum showed the triplet-quartet pattern characteristic for the ethyl protons at δ 1.20 and 4.03–4.16 ppm, respectively.

Regarding Scheme 5, reaction of **12** with carbon disulfide in ethanol at room temperature in the presence of potassium hydroxide afforded the potassium hydrazine-1-carbodithioate

derivative **19**. ^{13}C NMR spectrum of this compound showed three characteristic signals at δ 161.2, 172.8 and 187.6 ppm corresponding to two (C=O) and (C=S) carbons, respectively. On the other hand, heating **12** with carbon disulfide in ethanol in the presence of potassium hydroxide underwent cyclization to afford [1,3,4]oxadiazole-5-thione analog **20**. The spectroscopic data of compound **20** were consistent with its structure. For example, ^{13}C



Scheme 5. Synthesis of compounds 19–24.

NMR spectrum showed a characteristic signal at δ 183.4 ppm corresponding to (C=S) carbon. In addition, HRMS exhibited a significant peak at m/z $[M-H]^-$ 334.9551 which is in agreement with its molecular formula $C_{12}H_4ClN_4O_2S_2$. Heating **19** or **20** with hydrazine hydrate in ethanol resulted in the formation of compound **21**. 1H NMR spectrum of this compound showed two significant singlets at δ 4.15 and 12.55 ppm indicating (NH₂) and (NH) groups, respectively. When compound **12** was allowed to react with phenyl isothiocyanate in ethanol, 2-(8-chloro-2-oxo-2H-pyrimido[2,1-*b*]benzothiazole-4-carbonyl)-*N*-(phenyl)hydrazine-1-carbothioamide (**22**) was obtained. 1H NMR spectrum of **22** showed three singlets at δ 10.20, 11.78 and 13.63 ppm corresponding to three (NH) groups. Furthermore, ^{13}C NMR spectrum of the same compound showed a significant signal at δ 187.7 ppm corresponding to (C=S) carbon. Heating **22** in pyridine produced 5-phenylamino-[1,3,4]oxadiazole derivative **23**. On the other hand, cyclization of **22** into the corresponding 5-phenylamino-[1,3,4]thiadiazole derivative **24** was accomplished *via* its stirring with concentrated sulfuric acid at room temperature. HRMS of compound **24** revealed a peak at m/z $[M-H]^-$ 410.0023 which is in agreement with its molecular formula $C_{18}H_9ClN_5OS_2$.

3.2. Antitumor screening

3.2.1. Preliminary *in vitro* antitumor screening

Out of the newly synthesized compounds, nineteen derivatives, **4–10** and **13–24** were selected by the National Cancer Institute (NCI) *in vitro* disease-oriented human cells screening panel assay to be evaluated for their antitumor activity in accordance with the current protocol of the Drug Evaluation Branch, NCI, Bethesda [49–51]. A single dose (10 μ M) of the tested compounds was used in the full NCI-60 cell lines panel assay which includes nine tumor subpanels; namely, leukemia, non-small cell lung, colon, CNS,

melanoma, ovarian, renal, prostate and breast cancer cells. The data reported as mean-graph of the percentage growth of the treated cells, and presented as percentage growth inhibition (GI%). The obtained results of the tested compounds (Tables 1 and 2) showed distinctive potential pattern of selectivity as well as broad spectrum antitumor activity. The mean inhibition percentages for each of the tested compounds over the full panel of cell lines are illustrated in Fig. 4.

Regarding the activity toward individual cell lines, compounds **4**, **10**, **14** and **17** exhibited lethal effects (>100% inhibition) against nearly all tested leukemia cell lines, whereas compounds **4** and **17** displayed promising activity against almost all colon, melanoma, renal and breast cancer cell lines. In addition, compounds **4**, **10** and **17** exhibited excellent activity against most of the tested ovarian cancer cell lines. Close examination of the data presented in Tables 1 and 2, revealed that compounds **4** and **17** are the most active members in this study, showing lethal effects against numerous cell lines belonging to different tumor subpanels. The percentage inhibition of compounds **4** and **17** over each cell line of the NCI-60 cell lines panel is illustrated in Fig. 5. The six most active compounds, **4**, **6**, **10**, **14**, **17** and **20** passed this primary anticancer assay and consequently they were carried over to the five dose screen against a panel of about 60 cancer cell lines. Results indicated that these compounds possess considerable activity against non-small cell lung cancer (NCI-H522), colon cancer (HCT-116, HCT-15 and HT29) and breast cancer (MDA-MB-468 and MDA-MB-231/ATCC) cell lines in which EGFR is overexpressed in varying levels. These results support the postulation that these compounds may act *via* inhibition of EGFR-TK. Moreover, the broad spectrum activity of compound **4** against various cell lines encouraged further investigation of its inhibitory activity of additional targets. Previously, we examined compound **4** over EGFR-TK as well as other 10 different human kinases. Results indicated that compound

Table 1
Percentage growth inhibition (GI %) of compounds **4–10** at concentration (10 μ M) over *in vitro* subpanel tumor cell lines.

Subpanel tumor cell lines	% Growth inhibition (GI %) ^a						
	4	5	6	7	8	9	10
Leukemia							
CCRF-CEM	L	5.9	L	19.7	22.4	38.3	L
HL-60 (TB)	L	–	L	7.5	3.0	13.4	L
K-562	L	8.5	35.1	9.7	6.3	44.0	96.5
MOLT-4	L	8.0	55.6	9.7	–	65.1	L
RPMI-8226	L	7.1	51.0	13.5	24.4	38.0	L
SR	L	10.6	76.8	3.6	0.91	51.1	L
Non-small cell lung cancer							
A549/ATCC	L	3.5	22.0	9.5	10.2	16.0	39.8
HOP-62	L	8.6	13.4	–	7.0	12.0	55.4
HOP-92	nt	nt	nt	49.0	73.9	nt	nt
NCI-H226	L	18.6	5.2	14.2	21.0	15.7	64.2
NCI-H23	L	nt	nt	9.0	6.6	nt	nt
NCI-H322M	92.3	2.2	–	7.6	6.4	23.2	–
NCI-H460	L	4.4	0.8	10.2	0.69	8.7	48.7
NCI-H522	L	7.3	L	12.9	4.9	42.8	L
Colon cancer							
COLO 205	L	–	–	–	–	–	79.1
HCC-2998	L	–	–	56.3	–	10.0	65.6
HCT-116	L	7.0	11.5	–	1.3	33.2	84.0
HCT-15	L	7.5	18.0	6.5	3.7	27.0	84.7
HT29	L	–	94.7	–	–	36.3	95.8
KM 12	L	4.5	20.6	17.0	–	21.3	33.8
SW-620	L	2.3	9.1	–	–	0.36	79.3
CNS cancer							
SF-268	L	–	70.5	–	–	25.4	L
SF-295	L	7.2	2.3	2.1	21.3	28.2	24.1
SF-539	L	10.0	10.0	–	9.8	14.6	66.0
SNB-19	65.3	12.2	4.0	3.2	3.1	12.0	31.3
SNB-75	L	26.8	30.6	18.4	22.3	17.8	L
U251	L	7.3	0.8	10.1	8.9	16.8	58.1
Melanoma							
LOX IMVI	L	4.8	L	–	–	28.2	nt
M14	L	1.7	4.5	2.7	–	14.2	68.1
MDA-MB-435	L	–	–	–	12.5	9.0	58.5
SK-MEL-2	L	–	62.3	–	0.4	12.8	L
SK-MEL-28	L	–	–	–	0.67	–	27.0
SK-MEL-5	L	nt	nt	3.9	20.0	nt	nt
UACC-257	L	1.6	8.4	–	11.8	4.8	55.8
UACC-62	nt	6.4	8.3	16.5	32.5	35.5	74.0
Ovarian cancer							
IGORV1	L	–	L	16.7	11.4	33.0	L
OVCAR-3	L	2.25	24.5	–	–	18.4	L
OVCAR-4	L	16.7	–	55.0	8.5	23.7	L
OVCAR-5	L	13.2	3.5	19.2	–	20.9	38.7
OVCAR-8	L	3.4	37.5	6.5	9.9	21.5	73.2
NCI/ADR-RES	L	0.87	66.9	–	–	16.5	63.8
SK-OV-3	L	–	–	–	1.5	20.8	L
Renal cancer							
786-0	L	–	L	1.15	–	19.6	L
A498	91.3	11.3	–	23.3	20.7	52.0	10.6
ACHN	L	12.4	52.2	4.3	6.8	18.2	83.3
CAKI-1	L	19.6	65.6	32.3	30.6	28.3	92.0
RXF 393	nt	9.2	7.6	0.44	3.2	29.4	31.3
SN12C	L	4.2	3.7	6.8	21.3	19.5	53.1
UO-31	L	31.5	L	36.1	40.2	49.7	L
Prostate cancer							
PC-3	81.7	20.4	15.6	18.6	4.9	46.5	43.9
DU-145	L	–	2.8	–	–	9.0	22.5
Breast cancer							
MCF-7	L	18.0	3.7	91.4	16.4	33.6	79.0
MDA-MB-231/ATCC	L	15.4	34.9	27.3	6.6	42.7	94.8
HS 578T	L	3.9	–	10.6	10.3	36.3	56.0
BT-549	L	–	–	–	6.2	29.7	L
MDA-MB-468	L	8.3	20.0	nt	nt	23.6	L
T-47D	L	nt	L	63.4	15.4	nt	nt

Bold values used to point out the active compounds and lethal effect.

^a –, Percentage growth >100%; nt, not tested; L, lethal.

4 has moderate selectivity against EGFR-TK [48]. It is worth mentioning that the ongoing biological screening of compound **4** will shed the light on its broad spectrum antitumor activity.

3.2.1.1. Structure–activity relationship (SAR) studies. Structure activity correlation based on the number of cell lines that were proved to be sensitive toward each of the tested compounds is discussed:

Concerning compounds **4–10**, combination of the pyrazole moiety with the benzothiazole nucleus increased the antitumor activity (compounds **4**, **6**, **9** and **10**). The presence of 2-hydroxy ester substituents on the pyrazole ring (compound **4**) greatly enhanced the antitumor activity against all tested cancer cell lines compared to the 2-amino ester analog (compound **5**). In addition, replacement of the ester group at 4-position of the pyrazole moiety with the cyano group increased the antitumor activity against most of the tested cancer cell lines (compare **6** versus **5**). Compound **8** containing 3,5-dioxypyrazole moiety exhibited higher activity against most of the tested cancer cell lines compared to compound **7** containing 3-methyl-5-oxypyrazole moiety, this might be attributed to the additional hydrogen bonding site in compound **8**. Furthermore, replacement of 5-methyl substituent on the pyrazole moiety with 5-phenyl substituent in attempt to fit into the additional hydrophobic pocket of EGFR-TK active site resulted in higher antitumor activity (compound **10** versus **9**).

Taking into account the structure of pyrimido[2,1-*b*]benzothiazoles **13–24**, it is assumed that combination of 3-oxypyrazole moiety with the pyrimido[2,1-*b*]benzothiazole nucleus enhanced the antitumor activity over the other substituted pyrazole moieties (compounds **14** and **17** versus **13**, **15**, **16** and **18**). Furthermore, compound **16** containing 3-methyl-5-oxypyrazole moiety exhibited higher activity compared to compound **13** containing 3,5-dimethylpyrazole moiety, this might be attributed to the additional hydrogen bonding site in compound **16**. In addition, compound **14** containing 3,5-dioxypyrazole moiety exhibited higher activity against most of the tested cancer cell lines compared to compound **16** containing 3-methyl-5-oxypyrazole moiety, this might be attributed to the additional hydrogen bonding site in the 3,5-dioxypyrazole derivative **14**. Furthermore, combination of [1,3,4]oxadiazole moiety with the pyrimido[2,1-*b*]benzothiazole nucleus increased the activity over the analogs with [1,3,4]thiadiazole moiety (compare **20** and **23** versus **24**). Trials to improve the binding affinity toward the target receptor by promoting hydrogen bonding interaction of compound **20** via introducing an additional amino group to the bioisosteric [1,2,4]triazole derivative (compound **21**) or by favoring hydrophobic interaction via adding an extra phenyl moiety (compound **23**) resulted in decreased activity.

Comparing the antitumor activity of benzothiazole derivatives **4**, **5**, **7** and **9** with that of the corresponding pyrimido[2,1-*b*]benzothiazole derivatives **18**, **15**, **16** and **13**, respectively, we can conclude that the benzothiazole derivatives have higher activity against most of the tested cancer cell lines than the corresponding pyrimido[2,1-*b*]benzothiazoles.

3.2.2. Full *in vitro* five dose antitumor assay

About 60 cell lines of nine tumor subpanels; namely, leukemia, non-small cell lung, colon, CNS, melanoma, ovarian, renal, prostate and breast cancer cell lines were incubated with five concentrations (0.01–100 μ M) for each compound and were used to create log concentration – % growth inhibition curves. Three response parameters (GI₅₀, TGI, and LC₅₀) were calculated for each cell line. The GI₅₀ value (growth inhibitory activity) corresponds to the concentration of the compounds causing 50% decrease in cell growth, the TGI value (cytostatic activity) is the concentration of the compounds resulting in total growth inhibition and the LC₅₀

Table 2
Percentage growth inhibition (GI %) of compounds **13–24** at concentration (10 μ M) over *in vitro* subpanel tumor cell lines.

Subpanel tumor cell lines	% Growth inhibition (GI %) ^a											
	13	14	15	16	17	18	19	20	21	22	23	24
Leukemia												
CCRF-CEM	9.7	L	5.2	11.0	L	14.8	13.3	87.5	10.4	8.5	38.4	40.6
HL-60 (TB)	–	L	–	3.5	L	10.9	–	89.1	0.7	–	19.0	9.2
K-562	1.9	75.7	–	11.3	L	32.6	13.2	86.2	2.0	8.3	50.4	18.1
MOLT-4	0.4	L	–	17.6	L	11.8	6.7	99.6	0.5	5.0	43.5	15.0
RPMI-8226	9.2	L	3.7	3.4	L	12.8	8.2	85.7	6.4	11.2	49.3	4.4
SR	–	L	9.1	22.6	L	11.0	14.5	86.2	–	12.0	71.2	10.8
Non-small cell lung cancer												
A549/ATCC	0.07	29.3	–	8.1	68.0	12.6	6.0	90.0	–	–	23.8	–
HOP-62	7.4	23.4	–	8.1	27.3	–	–	60.8	–	–	10.8	–
HOP-92	34.6	nt	nt	nt	nt	12.6	nt	nt	nt	nt	91.4	nt
NCI-H226	18.5	39.4	20.1	11.7	L	8.7	14.7	71.0	16.5	11.6	36.2	2.0
NCI-H23	3.8	nt	2.9	nt	nt	–	nt	nt	nt	nt	38.6	nt
NCI-H322M	–	5.2	6.1	6.5	27.9	10.3	0.36	63.8	13.5	5.7	15.7	2.0
NCI-H460	–	21.2	–	0.5	76.6	1.4	4.0	93.7	4.6	–	36.1	–
NCI-H522	4.5	L	0.15	26.5	L	20.0	13.4	L	7.4	13.7	41.2	41.1
Colon cancer												
COLO 205	3.7	35.5	–	–	L	–	–	4.1	–	–	–	–
HCC-2998	–	23.1	nt	–	L	–	–	59.7	–	–	18.7	–
HCT-116	1.2	61.8	6.8	12.3	L	–	2.0	90.4	–	1.5	58.0	7.1
HCT-15	–	53.5	5.0	5.6	L	18.2	12.0	80.5	–	5.3	38.0	12.0
HT29	–	90.6	–	5.2	L	–	6.1	28.5	–	–	50.4	7.0
KM 12	–	18.1	2.6	3.5	51.7	15.4	0.65	85.8	–	2.7	31.9	–
SW-620	–	49.5	–	–	L	–	–	70.5	–	–	31.0	2.6
CNS cancer												
SF-268	–	98.2	–	–	90.0	–	3.8	73.2	–	–	24.3	–
SF-295	11.5	21.1	–	2.5	1.8	2.7	nt	59.4	–	4.3	10.6	4.5
SF-539	3.2	22.3	4.1	–	L	11.5	0.78	76.4	–	3.7	17.1	–
SNB-19	0.11	14.5	6.5	10.1	49.2	6.8	12.3	80.2	–	9.1	5.6	9.0
SNB-75	20.5	L	0.64	–	58.7	15.9	0.17	58.2	17.1	5.7	14.0	5.4
U251	5.7	31.5	0.82	13.5	62.1	5.3	11.2	96.7	–	7.7	24.3	2.2
Melanoma												
LOX IMVI	0.36	L	–	6.6	L	–	4.5	nt	12.8	7.8	34.2	2.35
M14	–	40.0	1.62	1.8	L	–	0.95	74.7	–	–	11.9	0.49
MDA-MB-435	0.42	35.0	–	0.5	L	30.2	5.4	73.5	–	–	19.6	7.2
SK-MEL-2	2.0	L	–	0.3	L	0.19	0.34	81.6	–	1.35	16.7	–
SK-MEL-28	–	1.3	–	–	94.6	–	–	67.8	1.8	–	6.8	nt
SK-MEL-5	0.75	nt	9.9	nt	nt	–	nt	nt	nt	nt	27.9	nt
UACC-257	1.0	50.8	–	–	L	4.2	–	85.2	–	0.65	15.1	9.8
UACC-62	3.9	45.4	nt	–	L	6.1	6.85	95.8	–	4.45	41.5	5.4
Ovarian cancer												
IGORV1	–	L	2.1	9.2	90.4	1.8	–	76.6	9.8	–	66.4	–
OVCAR-3	–	84.8	–	0.8	L	–	1.4	83.7	–	–	38.4	–
OVCAR-4	5.1	30.2	6.1	5.3	L	–	7.1	77.8	–	7.4	42.4	9.6
OVCAR-5	1.7	11.0	3.0	–	L	–	8.0	52.6	–	14.1	15.8	6.2
OVCAR-8	3.9	44.4	–	–	99.3	4.7	3.1	77.3	–	4.8	14.9	0.5
NCI/ADR-RES	–	41.3	–	–	89.2	–	–	84.0	–	–	22.8	–
SK-OV-3	0.8	71.3	–	–	51.7	0.49	–	42.0	3.0	–	12.2	–
Renal cancer												
786-0	–	69.1	3.7	7.8	L	–	–	58.3	0.80	0.34	15.3	6.1
A498	–	0.94	20.7	17.3	72.7	7.1	12.0	L	–	14.0	21.8	9.7
ACHN	5.8	35.5	3.9	0.1	L	13.3	8.5	88.2	4.8	4.0	39.4	7.4
CAKI-1	25.7	71.4	6.8	9.8	L	23.2	nt	90.8	11.2	11.3	46.0	1.5
RXF 393	1.9	27.1	nt	2.1	L	9.1	4.8	60.5	–	5.8	37.7	3.7
SN12C	14.4	30.8	2.4	–	L	6.2	7.5	84.3	2.0	2.1	–	0.25
UO-31	42.2	L	14.1	29.4	L	31.9	18.6	85.2	27.0	18.7	59.4	5.4
Prostate cancer												
PC-3	7.0	44.0	5.4	14.6	88.3	9.7	17.2	81.6	9.60	13.0	41.7	5.7
DU-145	–	10.5	–	–	L	–	–	73.0	–	–	9.3	–
Breast cancer												
MCF-7	2.1	61.5	7.6	11.5	L	15.2	9.6	91.0	8.3	14.2	55.6	9.4
MDA-MB-231/ATCC	–	66.2	–	–	L	22.5	–	86.7	18.3	8.7	67.8	–
HS 578T	2.3	28.1	–	3.0	85.2	–	–	70.2	4.2	–	24.5	–
BT-549	–	66.2	3.4	5.4	L	–	1.06	84.6	–	–	15.0	–
T-47D	9.6	nt	5.2	nt	nt	18.7	26.3	nt	8.2	nt	60.8	nt
MDA-MB-468	9.3	L	19.7	17.8	L	nt	nt	L	nt	7.5	nt	15.8

Bold values used to point out the active compounds and lethal effect.

^a –, Percentage growth >100%; nt, not tested; L, lethal.

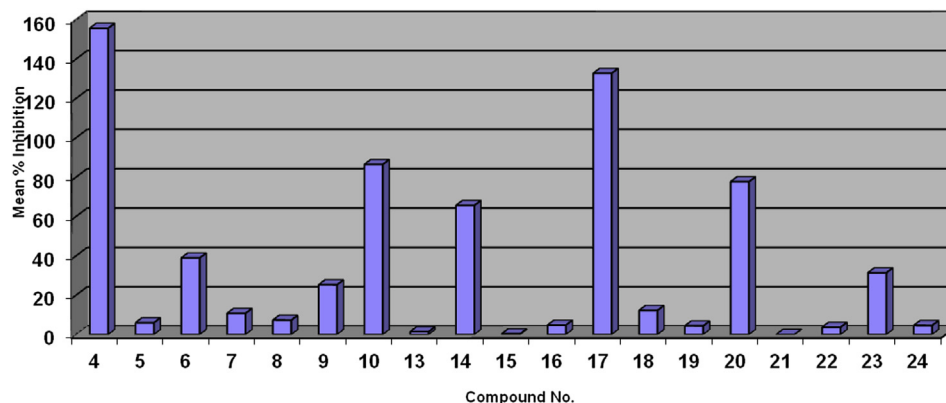


Fig. 4. Mean inhibition percentages of the tested compounds at concentration (10 μM) over the NCI-60 cancer cell lines. The inhibition percentages were calculated by subtracting the growth percentages from 100.

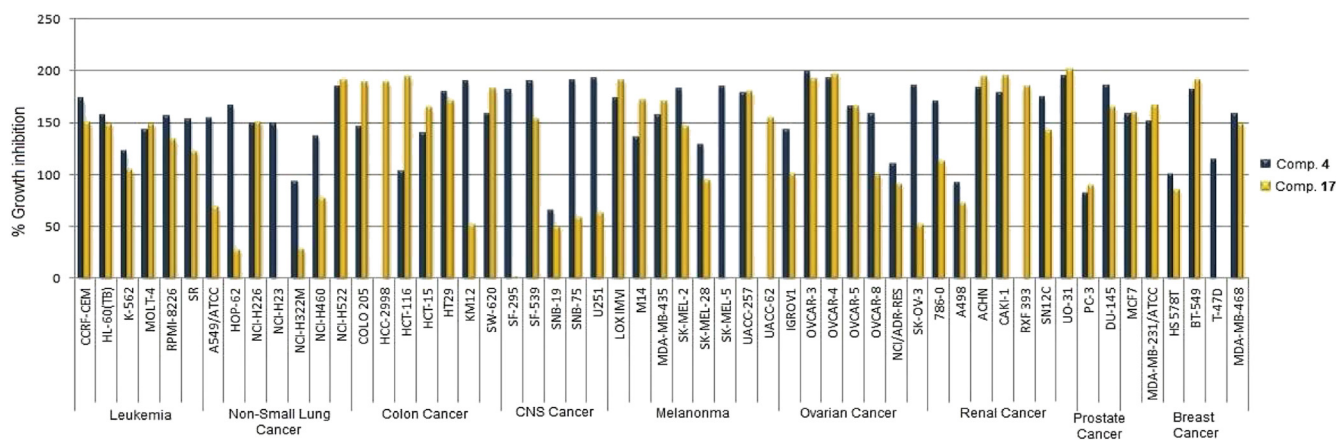


Fig. 5. % Growth inhibition expressed by compounds 4 and 17 at concentration (10 μM) over the NCI-60 cancer cell lines.

Table 3

Median growth inhibitory concentration (GI_{50} , μM) of the most active compounds over the most sensitive cell line of each tumor subpanel.

Comp. No.	Subpanel tumor cell lines								
	CCRF-CEM ^a	NCI-H522 ^b	HT29 ^c	SNB-75 ^d	LOX IMVI ^e	IGROV1 ^f	CAKI-1 ^g	PC-3 ^h	MDA-MB-468 ⁱ
4	0.182	0.0573	0.353	0.383	0.0319	0.152	0.548	0.749	0.56
6	0.24	0.191	2.4	1.61	0.199	0.378	2.62	2.12	4.17
10	0.0575	0.154	0.951	1.03	0.0175	0.202	0.0472	1.34	1.31
14	0.0338	0.0223	0.466	0.802	0.204	0.0428	1.06	0.575	1.87
17	0.124	0.145	0.284	1.11	0.179	1.47	0.256	0.553	0.148
20	2.71	2.43	3.46	1.20	2.7	2.29	1.82	2.13	0.0691

Bold values represent GI_{50} values in the nanomolar range.

^a Leukemia cell line.

^b Non-small cell lung cancer cell line.

^c Colon cancer cell line.

^d CNS cancer cell line.

^e Melanoma cell line.

^f Ovarian cancer cell line.

^g Renal cancer cell line.

^h Prostate cancer cell line.

ⁱ Breast cancer cell line.

value (cytotoxic activity) is the concentration of the compounds causing 50% loss of initial cells at the end of the incubation period (48 h). Full panel mean-graph midpoint values (MG-MID) for certain agents are the average of individual GI_{50} , TGI, or LC_{50} values of all cell lines.

In the present study, the six active compounds, **4**, **6**, **10**, **14**, **17** and **20** exhibited potential antitumor activity against most of the

tested subpanel cancer cell lines (GI_{50} , TGI and LC_{50} values < 100 μM). These compounds showed a distinctive pattern of sensitivity against some individual cell lines (Table 3) as well as broad spectrum antitumor activity (Tables 4 and 5).

Concerning the sensitivity against some individual cell lines (Table 3), compound **4** showed GI_{50} values of 0.0319 and 0.0573 μM against melanoma cancer (LOX IMVI) and non-small cell lung

cancer (NCI-H522) cell lines, respectively. In addition, compound **10** showed GI_{50} values of 0.0175, 0.0472 and 0.0575 μM against melanoma (LOX IMVI), renal cancer (CAKI-1) and leukemia (CCRF-CEM) cell lines, respectively. Furthermore, compound **14** showed GI_{50} values of 0.0223, 0.0338 and 0.0428 μM against non-small cell lung cancer (NCI-H522), leukemia (CCRF-CEM) and ovarian cancer (IGROV1) cell lines, respectively.

With regard to broad spectrum antitumor activity, the results revealed that the six active compounds, **4**, **6**, **10**, **14**, **17** and **20** have effective growth inhibition GI_{50} (MG-MID) values of 0.77, 6.02, 1, 1.04, 0.44 and 1.9 μM , respectively (Table 4), besides a cytostatic activity TGI (MG-MID) values of 2.08, 33.11, 2.63, 6.02, 1.2 and 8.3 μM , respectively (Table 5). In addition, compounds **4**, **10** and **17** exhibited moderate cytotoxic activity with LC_{50} (MG-MID) values of 11.74, 9.5 and 6.6 μM , respectively (Table 5). Further interpretation of the obtained data revealed that compounds **17** (GI_{50} = 0.44 μM , TGI = 1.2 μM and LC_{50} MG-MID = 6.6 μM) and **4** (GI_{50} = 0.77 μM , TGI = 2.08 μM and LC_{50} MG-MID = 11.74 μM) are the most active members in this study with promising antitumor activity against all the tested subpanel cancer cell lines at micromolar and sub-micromolar concentration levels. Moreover, both compounds revealed distinctive effectiveness against leukemia subpanel at both the GI_{50} (0.27 and 0.24 μM , respectively) and TGI levels (1.4 and 0.87 μM , respectively) (Tables 4 and 5).

3.3. 3D pharmacophore elucidation

A 3D pharmacophore is defined as a critical geometric arrangement of molecular features forming a necessary but not sufficient condition for biological activity [52].

3D and 2D pharmacophoric maps for the structural features of compounds **4** and **17** (the most active members in this study) were created by LigandScout software [53] and presented in Figs. 6 and 7, respectively. The investigated pharmacophoric features, included hydrogen bond donors and acceptors as directed vectors, positive and negative ionizable regions as well as lipophilic areas that are represented by spheres. 3D and 2D pharmacophoric maps for structural features of compounds **4** and **17** which provide the arrangement of the pharmacophore contours are presented in Figs. 6 and 7.

Moreover, alignment of the structural features of benzothiazole derivatives **4**, **6** and **10** revealed that these compounds possess similar arrangements of pharmacophoric characters. Furthermore, compound **6** displayed additional site for hydrogen bonding

Table 4

Mean GI_{50} values (μM) of the most active compounds over *in vitro* subpanel tumor cell lines.^a

Comp. No.	Subpanel tumor cell lines ^b									MG-MID ^c
	I	II	III	IV	V	VI	VII	VIII	IX	
4	0.27	0.99	1.29	1.01	1.1	1.36	0.93	1.16	1.08	0.77
6	2.95	17.5	13.4	4.4	23.4	11.4	9.07	8.11	11.58	6.02
10	1.02	1.55	1.52	1.8	1.5	1.19	0.97	1.93	1.34	1
14	1.02	1.88	1.86	2.13	1.9	1.74	1.71	1.77	1.62	1.04
17	0.24	1.01	0.51	1.11	0.61	0.81	0.37	0.54	0.55	0.44
20	3.01	2.21	2.38	2.5	2.61	2.26	2.24	2.88	0.89	1.9

Bold values represent the best GI_{50} values against subpanel I cancer cell lines and GI_{50} (μM) full panel mean-graph mid point.

^a Mean GI_{50} values were calculated by dividing the summation of GI_{50} values of the compound over cell lines of the same cancer type by the number of cell lines in the subpanel.

^b I: Leukemia; II: Non-Small Cell Lung Cancer; III: Colon Cancer; IV: CNS Cancer; V: Melanoma; VI: Ovarian Cancer; VII: Renal Cancer; VIII: Prostate Cancer; IX: Breast Cancer.

^c GI_{50} (μM) full panel mean-graph mid point (MG-MID) = the average sensitivity of all cell lines toward the test compounds.

interaction through hydrogen bond donors which are represented by red spheres, while compound **10** incorporates an extra hydrophobic feature represented by yellow (in web version) sphere (Fig. 8).

Similarly, the pharmacophoric map which was based on alignment of the structural features of pyrimido[2,1-*b*]benzothiazole derivatives **14**, **17** and **20** demonstrated the resemblance of the geometric arrangement of their molecular features (Fig. 9).

4. Conclusion

In conclusion, new series of benzothiazole and pyrimido[2,1-*b*]benzothiazole derivatives were synthesized. The most active compounds, **4**, **6**, **10**, **14**, **17** and **20** displayed broad spectrum antitumor activity against most of the tested subpanel cancer cell lines at the GI_{50} and TGI levels, together with a mild to moderate cytotoxic (LC_{50}) activity. In addition, these compounds exhibited promising antitumor activity against several cancer cell lines, including colon cancer (HT29), non-small cell lung (NCI-H522), and breast cancer (MDA-MB-468) cell lines that overexpress epidermal growth factor receptor (EGFR); thus, these compounds need further study to explore their mechanism of antitumor activity. The benzothiazole derivative **4** and pyrimido[2,1-*b*]benzothiazole derivative **17** are considered to be the most active members in this study exhibiting remarkable growth inhibitory activity, cytostatic and cytotoxic activities. These preliminary encouraging results of biological screening of the newly synthesized compounds could offer an excellent framework in this field that may lead to the discovery of new potent antitumor agents.

5. Experimental

5.1. Chemistry

All melting points ($^{\circ}\text{C}$) were recorded on Fisher-Johns melting point apparatus and are uncorrected. The infrared spectra were recorded using Nicolet Magna-IR Fourier-Transform 560 Spectrometer (ν in cm^{-1}) at the Department of Chemistry, Georgia State University, USA. Nuclear magnetic resonance (^1H and ^{13}C NMR) spectra were obtained on Bruker Avance 400 MHz spectrometer using CDCl_3 and $\text{DMSO}-d_6$ as solvents at the Department of Chemistry, Georgia State University, USA. The chemical shifts are expressed in δ ppm using tetramethylsilane (TMS) as internal reference. Mass spectra were recorded on nano LC-Q-TOF micro (Waters Micromass) spectrometer in positive or negative ion mode as necessary at the Department of Chemistry, Georgia State University, USA. Microanalyses (C, H, N) were performed at the Department of Chemistry, Georgia State University, and were in agreement with the proposed structures. Reaction times were monitored using TLC plates, Silica gel 60 F254 precoated (E. Merck) and the spots were visualized by UV (366 nm). Chloroform:methanol (9:1) was adopted as an elution solvent. Compounds **2**, **3**, **11** and **12** were prepared adopting the reported procedure [7].

5.1.1. Ethyl 1-[2-((6-chlorobenzothiazol-2-yl)amino)-2-oxoethyl]-5-hydroxy-1H-pyrazole-4-carboxylate (**4**)

A mixture of compound **3** (0.257 g, 0.001 mol), diethyl ethoxymethylenemalonate (0.216 g, 0.001 mol) and anhydrous potassium carbonate (0.207 g, 0.0015 mol) in acetonitrile (15 mL) was heated under reflux for 12 h. After cooling, the solution was acidified with dilute hydrochloric acid and the precipitated dark yellow solid was collected by filtration, dried and crystallized from ethanol.

Table 5
Mean total growth inhibitory concentration (TGI, μM) and median lethal concentration (LC_{50} , μM) of the most active compounds over *in vitro* subpanel tumor cell lines.^a

Comp. No.	Subpanel tumor cell lines ^b									MG-MID ^e (MG-MID) ^f
	I	II	III	IV	V	VI	VII	VIII	IX	
4	1.4^c (–) ^d	1.9 (37.5)	3.4 (5.8)	2.5 (52.1)	2.97 (5.5)	2.6 (52.7)	2.06 (4.4)	2.9 (5.5)	2.5 (52.8)	2.08 (11.74)
6	51.5 (–)	51.4 (–)	59.4 (–)	40.9 (–)	86.1 (–)	67.9 (–)	40.7 (–)	46.1 (85.3)	26.9 (–)	33.11 (93.3)
10	2.6 (–)	4.8 (18.7)	3.34 (7.2)	5.14 (5.8)	3.2 (18.8)	3.2 (16.1)	2.4 (6.6)	5.2 (16.9)	4.6 (36.1)	2.63 (9.5)
14	25.8 (–)	28.5 (79.1)	23.2 (–)	20.2 (68.4)	22.3 (93.8)	24.3 (72.1)	9.1 (51.2)	9.2 (67.4)	20.8 (–)	6.02 (56.2)
17	0.87 (–)	2.3 (4.8)	1.1 (3.1)	2.5 (24.1)	1.4 (3.9)	2.1 (4.5)	1.1 (2.9)	1.8 (4.7)	2.1 (76.6)	1.2 (6.6)
20	13.4 (92.9)	8.5 (47.2)	9.1 (35.1)	20.9 (45.9)	9.5 (42.9)	10.7 (66.5)	7.7 (34.2)	11.3 (81.4)	4.8 (81.7)	8.3 (44.6)

^a Mean TGI and LC_{50} values were calculated by dividing the summation of TGI and LC_{50} values of the compound over cell lines of the same cancer type by the number of cell lines in the subpanel.

^b For subpanel tumor cell lines, see footnote (b) of Table 4.

^c Bold values represent the best mean TGI and LC_{50} values against subpanel tumor cell lines: I; III; V and VII.

^d Mean LC_{50} values are shown in parentheses, (–) for values > 100 μM .

^e TGI (μM) full panel mean-graph mid point (MG-MID) = the average sensitivity of all cell lines toward the test compounds.

^f LC_{50} (μM) full panel mean-graph mid point (MG-MID) = the average sensitivity of all cell lines toward the test compounds.

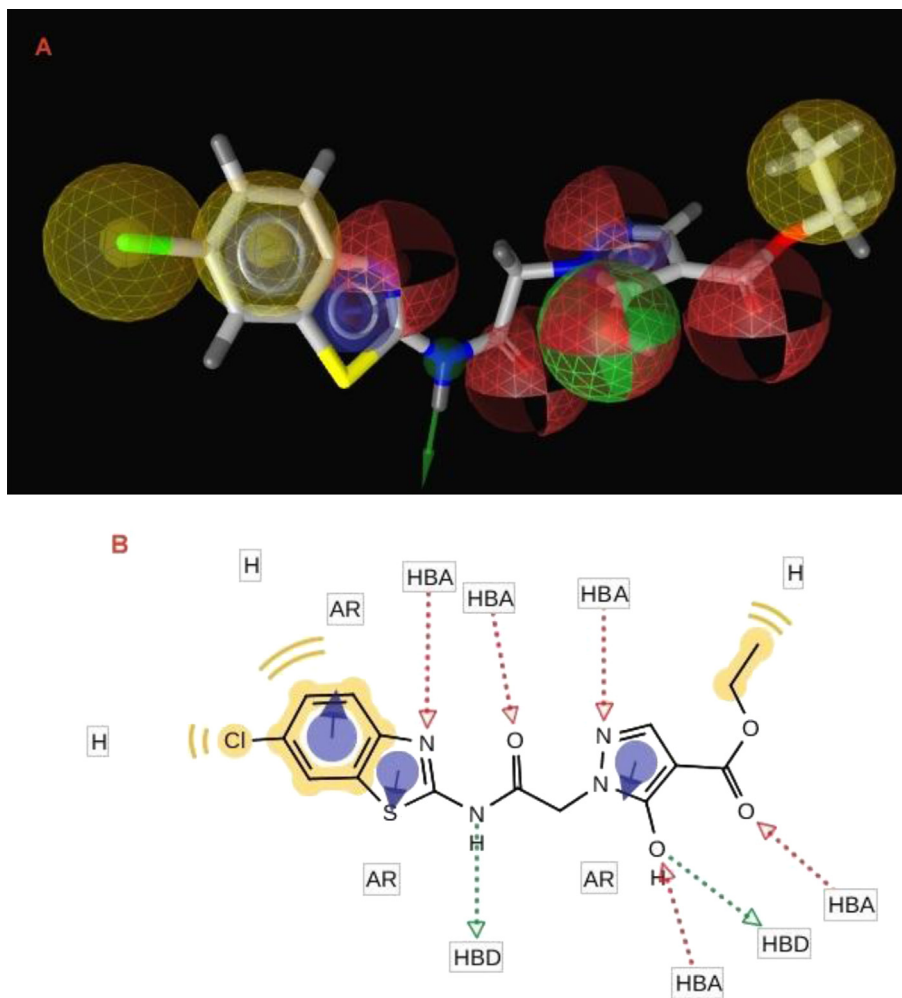


Fig. 6. The 3D and 2D pharmacophoric maps of compound **4**: (A) The 3D pharmacophoric map of compound **4**. The pharmacophore color coding is red for hydrogen acceptor, yellow for hydrophobic regions and green for hydrogen donors, (B) The 2D pharmacophoric map of compound **4**. HBA, hydrogen bond acceptor; H, hydrophobic center; HBD, hydrogen bond donor; AR, aryl. (For interpretation of the references to color in this figure legend, the reader is referred to the web version of this article.)

Yield 45%, m.p. 195–196 °C. IR (KBr, ν , cm^{-1}): 3260 (OH), 3150 (NH), 1710 ($\text{C}=\text{O}$), 1685 ($\text{C}=\text{O}$). ^1H NMR: (CDCl_3 , δ ppm): 1.30 (t, 3H, CH_2CH_3), 3.55 (s, 2H, COCH_2NH), 4.05–4.35 (q, 2H, CH_2CH_3), 7.20–7.80 (m, 4H, Ar–H, pyrazole–H), 10.40 (s, 1H, OH), 11.50 (s, 1H, NH). ^{13}C NMR: (CDCl_3 , δ ppm): 14.6 (CH_2CH_3), 56.9 (COCH_2NH), 61.0 (CH_2CH_3), 95.8 (pyrazole C-4), 121.0, 125.8, 128.0, 132.0, 135.5, 145.8, 157.2, 169.7 (Ar–C), 161.4 ($\text{C}=\text{O}$), 167.2 ($\text{C}=\text{O}$). HRMS: m/z (ESI) calcd. for $\text{C}_{15}\text{H}_{12}\text{ClN}_4\text{O}_4\text{S}^-$, $[\text{M}-\text{H}]^-$: 379.0346; found: 379.0352.

Anal. calcd. for $\text{C}_{15}\text{H}_{13}\text{ClN}_4\text{O}_4\text{S}$ (380.81): C, 47.31; H, 3.44; N, 14.71%. Found: C, 47.56; H, 3.25; N, 14.47%.

5.1.2. Ethyl 5-amino-1-[2-((6-chlorobenzothiazol-2-yl)amino)-2-oxoethyl]-1H-pyrazole-4-carboxylate (**5**)

A mixture of compound **3** (0.257 g, 0.001 mol), ethyl ethoxymethylenecyanoacetate (0.169 g, 0.001 mol) and anhydrous potassium carbonate (0.207 g, 0.0015 mol) in ethanol (15 mL) was

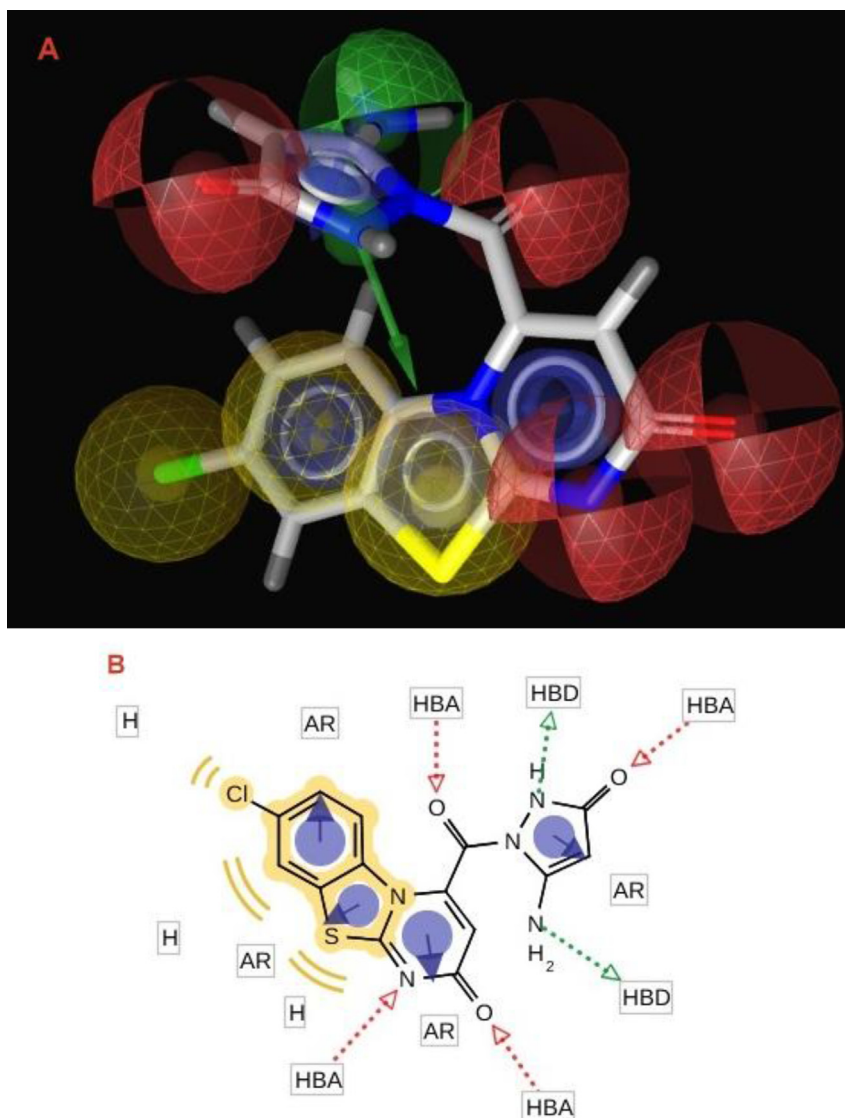


Fig. 7. The 3D and 2D pharmacophoric maps of compound **17**: (A) The 3D pharmacophoric map of compound **17**. The pharmacophore color coding is red for hydrogen acceptor, yellow for hydrophobic regions and green for hydrogen donors, (B) The 2D pharmacophoric map of compound **17**. HBA, hydrogen bond acceptor; H, hydrophobic center; HBD, hydrogen bond donor; AR, aryl. (For interpretation of the references to color in this figure legend, the reader is referred to the web version of this article.)

heated under reflux for 10 h. The solution was acidified with dilute hydrochloric acid and the precipitated yellow solid was collected by filtration, dried and crystallized from ethanol.

Yield 59%, m.p. 203–205 °C. IR (KBr, ν , cm^{-1}): 3315, 3210 (NH_2 , NH), 1715 (COOC_2H_5), 1675 ($\text{C}=\text{O}$). ^1H NMR: (DMSO- d_6 , δ ppm): 1.30 (t, 3H, CH_2CH_3), 3.85 (s, 2H, COCH_2NH), 4.28–4.35 (q, 2H, CH_2CH_3), 6.40 (s, 1H, pyrazole-H), 7.25–8.25 (m, 5H, Ar-H, NH_2), 11.40 (s, 1H, NH). ^{13}C NMR: (DMSO- d_6 , δ ppm): 15.0 (CH_2CH_3), 59.1 (COCH_2NH), 59.6 (CH_2CH_3), 118.5, 119.9, 120.1, 121.2, 126.1, 134.2, 150.6, 152.0, 163.7, 176.0 (Ar-C), 167.1 ($\text{C}=\text{O}$), 167.7 ($\text{C}=\text{O}$). HRMS: m/z (ESI) calcd. for $\text{C}_{15}\text{H}_{13}\text{ClN}_5\text{O}_3\text{S}^-$, $[\text{M}-\text{H}]^-$: 378.0506; found: 378.0512. Anal. calcd. for $\text{C}_{15}\text{H}_{14}\text{ClN}_5\text{O}_3\text{S}$ (379.82): C, 47.43; H, 3.72; N, 18.44%. Found: C, 47.16; H, 3.62; N, 18.67%.

5.1.3. 2-(5-Amino-4-cyano-1H-pyrazol-1-yl)-N-(6-chlorobenzothiazol-2-yl)acetamide (**6**)

A mixture of compound **3** (0.257 g, 0.001 mol), ethoxymethylenemalononitrile (0.122 g, 0.001 mol) and anhydrous potassium carbonate (0.207 g, 0.0015 mol) in ethanol (15 mL) was

heated under reflux for 8 h. The solvent was evaporated under reduced pressure and the remaining solid was crystallized from ethanol.

Yield 49%, m.p. 187–189 °C. IR (KBr, ν , cm^{-1}): 3260, 3160 (NH_2 , NH), 2215 ($\text{C}\equiv\text{N}$), 1674 ($\text{C}=\text{O}$). ^1H NMR: (DMSO- d_6 , δ ppm): 3.95 (s, 2H, CH_2), 5.25 (s, 2H, NH_2), 7.35–8.15 (m, 4H, Ar-H, pyrazole-H), 11.35 (s, 1H, NH). ^{13}C NMR: (DMSO- d_6 , δ ppm): 63.0 (CH_2), 80.8 (pyrazole C-4), 117.1 ($\text{C}\equiv\text{N}$), 119.0, 122.5, 126.0, 131.9, 135.6, 144.7, 161.2, 166.3, 181.8 (Ar-C), 168.6 ($\text{C}=\text{O}$). HRMS: m/z (ESI) calcd. for $\text{C}_{13}\text{H}_8\text{ClN}_6\text{OS}^-$, $[\text{M}-\text{H}]^-$: 331.0247; found: 331.0254. Anal. calcd. for $\text{C}_{13}\text{H}_9\text{ClN}_6\text{OS}$ (332.77): C, 46.92; H, 2.73; N, 25.25%. Found: C, 47.18; H, 2.89; N, 24.97%.

5.1.4. N-(6-Chlorobenzothiazol-2-yl)-2-(3-methyl-5-oxo-4,5-dihydro-1H-pyrazol-1-yl)acetamide (**7**)

A mixture of compound **3** (0.257 g, 0.001 mol), ethyl acetoacetate (0.13 g, 0.001 mol) and anhydrous potassium carbonate (0.207 g, 0.0015 mol) in ethanol (15 mL) was heated under reflux for 10 h. The reaction mixture was cooled and the precipitated

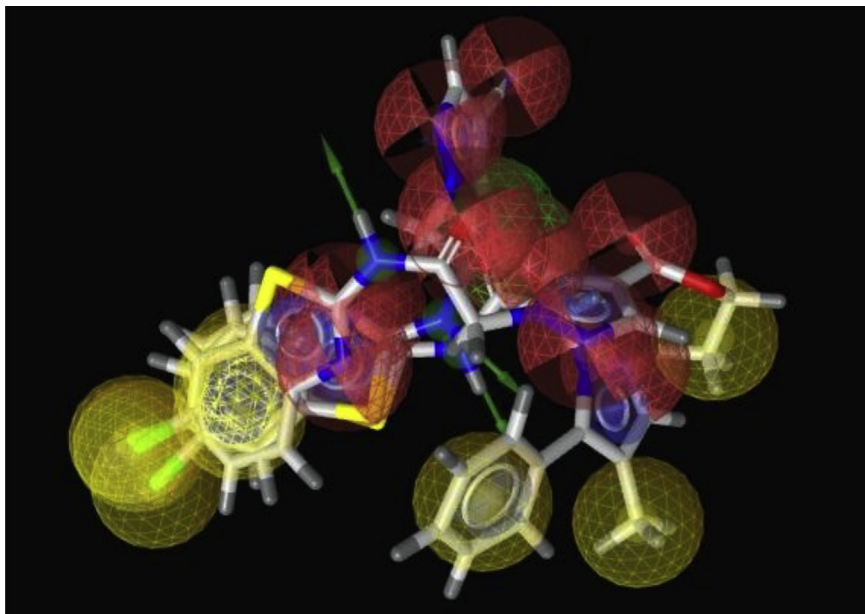


Fig. 8. The 3D alignment of the pharmacophoric features of benzothiazole derivatives **4**, **6** and **10**.

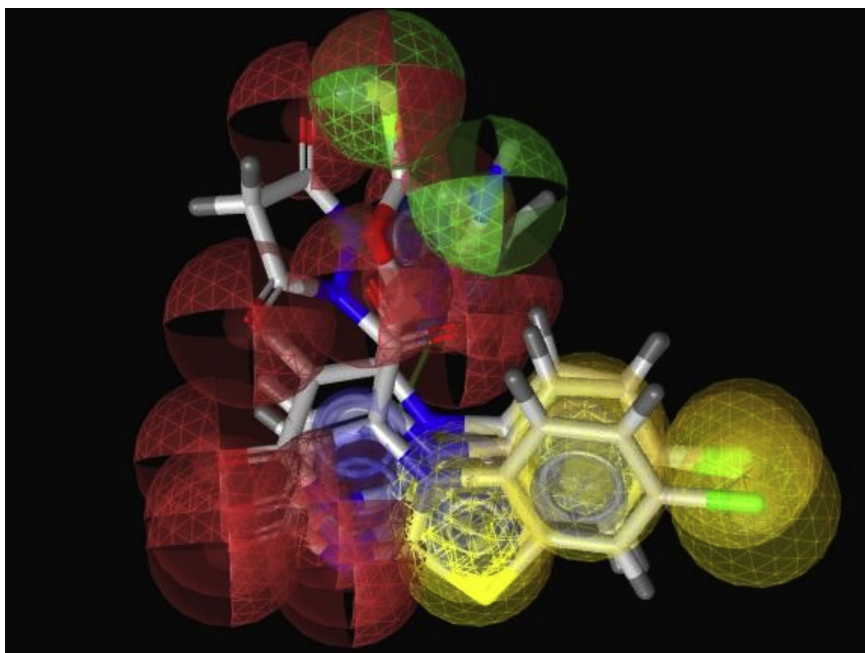


Fig. 9. The 3D alignment of the pharmacophoric features of pyrimido[2,1-*b*]benzothiazole derivatives **14**, **17** and **20**.

green solid was collected by filtration, washed with water, dried and crystallized from ethanol.

Yield 55%, m.p. 195–197 °C. IR (KBr, ν , cm^{-1}): 3277 (NH), 1710, 1674 (C=O). ^1H NMR: (DMSO- d_6 , δ ppm): 1.80 (s, 3H, CH_3), 4.20 (s, 2H, pyrazoline-H), 4.90 (s, 2H, CH_2), 7.20–7.70 (m, 3H, Ar-H), 11.50 (s, 1H, NH). ^{13}C NMR: (DMSO- d_6 , δ ppm): 22.5 (CH_3), 43.4 (CH_2), 56.0 (CH_2), 119.0, 121.0, 125.0, 126.2, 133.0, 152.1, 180.0 (Ar-C), 167.6 (C=O), 176.5 (C=O). HRMS: m/z (ESI) calcd. for $\text{C}_{13}\text{H}_{10}\text{ClN}_4\text{O}_2\text{S}^-$, $[\text{M}-\text{H}]^-$: 321.0291; found: 321.0298. Anal. calcd. for $\text{C}_{13}\text{H}_{11}\text{ClN}_4\text{O}_2\text{S}$ (322.77): C, 48.37; H, 3.44; N, 17.36%. Found: C, 48.69; H, 3.62; N, 17.15%.

5.1.5. *N*-(6-Chlorobenzothiazol-2-yl)-2-(3,5-dioxopyrazolidin-1-yl)acetamide (**8**)

A mixture of compound **3** (0.257 g, 0.001 mol) and diethyl malonate (0.641 g, 0.004 mol) was heated at 200 °C in an oil bath for 2 h then cooled. The obtained residue was triturated with diethyl ether and filtered. The filtrate was evaporated and the obtained solid was dried and crystallized from ethanol.

Yield 41%, m.p. 165–167 °C. IR (KBr, ν , cm^{-1}): 3150 (2NH), 1720, 1686, 1654 (3C=O). ^1H NMR: (DMSO- d_6 , δ ppm): 2.90 (s, 2H, pyrazolidine-H), 5.00 (s, 2H, CH_2), 7.30–8.20 (m, 3H, Ar-H), 11.60 (s, 1H, NH), 12.10 (s, 1H, NH). ^{13}C NMR: (DMSO- d_6 , δ ppm): 53.7

(CH₂), 60.8 (CH₂), 121.8, 122.1, 126.8, 127.9, 133.6, 147.9, 174.3 (Ar–C), 159.3 (C=O), 170.1 (C=O), 171.9 (C=O). HRMS: *m/z* (ESI) calcd. for C₁₂H₈ClN₄O₃S[−], [M–H][−]: 323.0084; found: 323.0089.

5.1.6. *N*-(6-Chlorobenzothiazol-2-yl)-2-(3,5-dimethyl-1*H*-pyrazol-1-yl)acetamide (**9**)

A mixture of compound **3** (0.257 g, 0.001 mol) and acetylacetone (0.1 g, 0.001 mol) in glacial acetic acid (15 mL) was heated under reflux for 10 h. The reaction mixture was cooled and the precipitated green solid was collected by filtration, washed with water, dried and crystallized from ethanol.

Yield 41%, m.p. 153–154 °C. IR (KBr, *v*, cm^{−1}): 3215 (NH), 1670 (C=O). ¹H NMR: (DMSO-*d*₆, *δ* ppm): 2.05 (s, 3H, CH₃), 2.25 (s, 3H, CH₃), 5.15 (s, 2H, CH₂), 7.35–8.15 (m, 4H, Ar–H, pyrazole-H), 12.45 (s, 1H, NH). ¹³C NMR: (DMSO-*d*₆, *δ* ppm): 20.7 (CH₃), 23.2 (CH₃), 63.2 (CH₂), 101.8 (pyrazole C-4), 121.9, 122.1, 126.9, 127.9, 133.6, 136.0, 147.9, 159.3, 174.5 (Ar–C), 167.9 (C=O). HRMS: *m/z* (ESI) calcd. for C₁₄H₁₂ClN₄O₃S[−], [M–H][−]: 319.0497; found: 319.0499.

5.1.7. *N*-(6-Chlorobenzothiazol-2-yl)-2-(3-methyl-5-phenyl-1*H*-pyrazol-1-yl)acetamide (**10**)

A mixture of compound **3** (0.257 g, 0.001 mol) and benzoylacetone (0.162 g, 0.001 mol) in glacial acetic acid (15 mL) was heated under reflux for 8 h. The solvent was evaporated under reduced pressure and the remaining solid was crystallized from ethanol.

Yield 66%, m.p. 201–203 °C. IR (KBr, *v*, cm^{−1}): 3297 (NH), 1658 (C=O). ¹H NMR: (DMSO-*d*₆, *δ* ppm): 1.90 (s, 3H, CH₃), 5.20 (s, 2H, CH₂), 7.45–8.20 (m, 9H, Ar–H, pyrazole-H), 12.40 (s, 1H, NH). ¹³C NMR: (DMSO-*d*₆, *δ* ppm): 21.5 (CH₃), 60.0 (CH₂), 115.5 (pyrazole C-4), 118.4, 121.8, 122.1, 126.8, 126.9, 127.9, 129.9, 133.6, 134.9, 147.8, 159.2, 172.4 (Ar–C), 170.1 (C=O). HRMS: *m/z* (ESI) calcd. for C₁₉H₁₄ClN₄O₃S[−], [M–H][−]: 381.0655; found: 381.0661. Anal. calcd. for C₁₉H₁₅ClN₄O₃S (382.87): C, 59.60; H, 3.95; N, 14.63%. Found: C, 59.36; H, 3.84; N, 14.82%.

5.1.8. 8-Chloro-4-(3,5-dimethyl-1*H*-pyrazole-1-carbonyl)-2*H*-pyrimido[2,1-*b*]benzothiazol-2-one (**13**)

A mixture of compound **12** (0.295 g, 0.001 mol) and acetylacetone (0.1 g, 0.001 mol) in glacial acetic acid (15 mL) was heated under reflux for 10 h. The reaction mixture was cooled and the precipitated green solid was collected by filtration, washed with water, dried and crystallized from ethanol.

Yield 49%, m.p. 186–188 °C. IR (KBr, *v*, cm^{−1}): 1675, 1660 (2C=O). ¹H NMR: (DMSO-*d*₆, *δ* ppm): 2.42 (s, 3H, CH₃), 2.95 (s, 3H, CH₃), 6.78–7.77 (m, 5H, Ar–H, pyrazole-H, pyrimidine-H). ¹³C NMR: (DMSO-*d*₆, *δ* ppm): 19.4 (CH₃), 20.2 (CH₃), 112.7, 117.6, 122.1, 122.3, 123.5, 126.9, 128.9, 137.1, 137.3, 163.5, 168.7 (Ar–C), 177.1 (C=O), 185.7 (C=O). HRMS: *m/z* (ESI) calcd. for C₁₆H₁₀ClN₄O₂S[−], [M–H][−]: 357.0291; found: 357.0298. Anal. calcd. for C₁₆H₁₁ClN₄O₂S (358.80): C, 53.56; H, 3.09; N, 15.61%. Found: C, 53.31; H, 3.26; N, 15.87%.

5.1.9. 1-(8-Chloro-2-oxo-2*H*-pyrimido[2,1-*b*]benzothiazole-4-carbonyl)pyrazolidine-3,5-dione (**14**)

A mixture of compound **12** (0.295 g, 0.001 mol) and diethyl malonate (0.641 g, 0.004 mol) was heated at 200 °C in an oil bath for 2 h then cooled. The obtained residue was triturated with diethyl ether and filtered. The filtrate was evaporated and the obtained solid was dried and crystallized from ethanol.

Yield 42%, m.p. 211–212 °C. IR (KBr, *v*, cm^{−1}): 3200 (NH), 1710, 1692, 1660, 1650 (4C=O). ¹H NMR: (DMSO-*d*₆, *δ* ppm): 4.15 (s, 2H, pyrazolidine-H), 6.80–8.25 (m, 4H, Ar–H, pyrimidine-H), 12.60 (s, 1H, NH). ¹³C NMR: (DMSO-*d*₆, *δ* ppm): 51.6 (pyrazolidine C-4), 119.0, 121.8, 122.4, 129.3, 129.5, 131.2, 143.2, 157.2, 162.8 (Ar–C), 162.9 (C=O), 170.9 (C=O), 171.1 (C=O), 176.0 (C=O). HRMS: *m/z* (ESI) calcd. for C₁₄H₆ClN₄O₄S[−], [M–H][−]: 360.9877; found: 360.9884.

5.1.10. Ethyl 5-amino-1-(8-chloro-2-oxo-2*H*-pyrimido[2,1-*b*]benzothiazole-4-carbonyl)-1*H*-pyrazole-4-carboxylate (**15**)

A mixture of compound **12** (0.295 g, 0.001 mol), ethyl ethoxymethylenecyanoacetate (0.169 g, 0.001 mol) and anhydrous potassium carbonate (0.207 g, 0.0015 mol) in ethanol (15 mL) was heated under reflux for 10 h. The solution was acidified with dilute hydrochloric acid and the precipitated yellow solid was collected by filtration, dried and crystallized from ethanol.

Yield 48%, m.p. 195–197 °C. IR (KBr, *v*, cm^{−1}): 3215, 3100 (NH₂), 1710 (COOC₂H₅), 1670, 1655 (2C=O). ¹H NMR: (DMSO-*d*₆, *δ* ppm): 1.23 (t, 3H, CH₂CH₃), 4.08–4.25 (q, 2H, CH₂CH₃), 6.42–7.78 (m, 4H, Ar–H, pyrimidine-H), 8.90 (s, 1H, pyrazole-H), 12.63 (s, 2H, NH₂). HRMS: *m/z* (ESI) calcd. for C₁₇H₁₁ClN₅O₄S[−], [M–H][−]: 416.0297; found: 416.0299.

5.1.11. 8-Chloro-4-(3-methyl-5-oxo-4,5-dihydro-1*H*-pyrazole-1-carbonyl)-2*H*-pyrimido[2,1-*b*]benzothiazol-2-one (**16**)

A mixture of compound **12** (0.295 g, 0.001 mol), ethyl acetoacetate (0.13 g, 0.001 mol) and anhydrous potassium carbonate (0.207 g, 0.0015 mol) in ethanol (15 mL) was heated under reflux for 10 h. The reaction mixture was cooled and the precipitated green solid was collected by filtration, washed with water, dried and crystallized from ethanol.

Yield 63%, m.p. 213–215 °C. IR (KBr, *v*, cm^{−1}): 1720, 1675 (3C=O). ¹H NMR: (DMSO-*d*₆, *δ* ppm): 2.15 (s, 3H, CH₃), 3.73 (s, 2H, pyrazoline-H), 6.45 (d, 1H, Ar–H), 6.85 (s, 1H, pyrimidine-H), 6.97 (d, 1H, Ar–H), 8.05 (s, 1H, Ar–H). ¹³C NMR: (DMSO-*d*₆, *δ* ppm): 20.2 (CH₃), 60.3 (pyrazoline C-4), 116.3, 122.8, 125.5, 127.2, 127.9, 128.1, 138.8, 153.3, 160.2, 163.4 (Ar–C, pyrazoline C-3), 163.5 (C=O), 168.7 (C=O), 184.0 (C=O). HRMS: *m/z* (ESI) calcd. for C₁₅H₈ClN₄O₃S[−], [M–H][−]: 359.0084; found: 359.0097.

5.1.12. 4-(5-Amino-3-oxo-2,3-dihydro-1*H*-pyrazole-1-carbonyl)-8-chloro-2*H*-pyrimido[2,1-*b*]benzothiazol-2-one (**17**)

A mixture of compound **12** (0.295 g, 0.001 mol) and ethyl cyanoacetate (0.113 g, 0.001 mol) in ethanol (15 mL) was heated under reflux for 10 h. The reaction mixture was cooled and the precipitated solid was collected by filtration, washed with water, dried and crystallized from ethanol.

Yield 48%, m.p. 145–147 °C. IR (KBr, *v*, cm^{−1}): 3300, 3210 (NH₂, NH), 1685, 1660 (3C=O). ¹H NMR: (DMSO-*d*₆, *δ* ppm): 5.75 (s, 1H, pyrazoline-H), 6.23 (s, 1H, pyrimidine-H), 7.13–7.86 (m, 5H, Ar–H, NH₂), 11.97 (s, 1H, NH). HRMS: *m/z* (ESI) calcd. for C₁₄H₇ClN₅O₃S[−], [M–H][−]: 360.0063; found: 360.0045.

5.1.13. Ethyl 1-(8-chloro-2-oxo-2*H*-pyrimido[2,1-*b*]benzothiazole-4-carbonyl)-5-hydroxy-1*H*-pyrazole-4-carboxylate (**18**)

A mixture of compound **12** (0.295 g, 0.001 mol), diethyl ethoxymethylenemalonate (0.216 g, 0.001 mol) and anhydrous potassium carbonate (0.207 g, 0.0015 mol) in acetonitrile (15 mL) was heated under reflux for 12 h. The solution was acidified with dilute hydrochloric acid and the precipitated dark yellow solid was collected by filtration, dried and crystallized from ethanol.

Yield 41%, m.p. 225–227 °C. IR (KBr, *v*, cm^{−1}): 3377 (OH), 1715 (COOC₂H₅), 1690, 1665 (2C=O). ¹H NMR: (DMSO-*d*₆, *δ* ppm): 1.20 (t, 3H, CH₂CH₃), 4.03–4.16 (q, 2H, CH₂CH₃), 7.15–8.20 (m, 6H, Ar–H, pyrazole-H, pyrimidine-H, OH). HRMS: *m/z* (ESI) calcd. for C₁₇H₁₀ClN₄O₅S[−], [M–H][−]: 417.0139; found: 417.0143. Anal. calcd. for C₁₇H₁₁ClN₄O₅S (418.81): C, 48.75; H, 2.65; N, 13.38%. Found: C, 48.93; H, 2.84; N, 13.49%.

5.1.14. Potassium 2-(8-chloro-2-oxo-2*H*-pyrimido[2,1-*b*]benzothiazole-4-carbonyl)hydrazine-1-carbodithioate (**19**)

A solution of potassium hydroxide (0.84 g, 0.015 mol) in water (10 mL) was added to a mixture of compound **12** (2.95 g, 0.01 mol)

and carbon disulfide (5 mL, excess) in ethanol (20 mL). The mixture was stirred at room temperature for 8 h. The precipitated dark yellow solid was collected by filtration, washed with water, dried and crystallized from ethanol.

Yield 65%, m.p. 167–169 °C. IR (KBr, ν , cm^{-1}): 3100 (2NH), 1690, 1655 (2C=O). ^1H NMR: (DMSO- d_6 , δ ppm): 7.05–7.65 (m, 3H, Ar-H), 8.20 (s, 1H, pyrimidine-H), 11.15 (s, 1H, NH), 12.65 (s, 1H, NH). ^{13}C NMR: (DMSO- d_6 , δ ppm): 108.3, 118.5, 121.2, 124.6, 126.5, 129.5, 138.7, 158.4, 161.2 (Ar-C), 161.5 (C=O), 172.8 (C=O), 187.6 (C=S). HRMS: m/z (ESI) calcd for $\text{C}_{12}\text{H}_5\text{ClKN}_4\text{O}_2\text{S}_3$, $[\text{M}-\text{H}]^-$: 406.8978; found: 406.8984.

5.1.15. 8-Chloro-4-(5-thioxo-4,5-dihydro-[1,3,4]oxadiazol-2-yl)-2H-pyrimido[2,1-b]benzothiazol-2-one (20)

A solution of potassium hydroxide (0.84 g, 0.015 mol) in water (10 mL) was added to a mixture of compound **12** (2.95 g, 0.01 mol) and carbon disulfide (5 mL, excess) in ethanol (20 mL). The mixture was heated under reflux for 10 h. The precipitated dark orange solid was collected by filtration, washed with water, dried and crystallized from ethanol.

Yield 51%, m.p. 190–192 °C. IR (KBr, ν , cm^{-1}): 3175 (NH), 1690 (C=O). ^1H NMR: (DMSO- d_6 , δ ppm): 6.95–7.35 (m, 3H, Ar-H), 8.25 (s, 1H, pyrimidine-H), 14.55 (s, 1H, NH). ^{13}C NMR: (DMSO- d_6 , δ ppm): 109.5, 114.8, 123.9, 127.9, 129.1, 132.1, 147.6, 157.0, 157.7, 172.4 (Ar-C, oxadiazole C-2), 178.6 (C=O), 183.4 (C=S). HRMS: m/z (ESI) calcd. for $\text{C}_{12}\text{H}_4\text{ClN}_4\text{O}_2\text{S}_2$, $[\text{M}-\text{H}]^-$: 334.9542; found: 334.9551.

5.1.16. 4-(4-Amino-5-thioxo-4,5-dihydro-1H-[1,2,4]triazol-3-yl)-8-chloro-2H-pyrimido[2,1-b]benzothiazol-2-one (21)

5.1.16.1. Method A. A mixture of compound **19** (0.409 g, 0.001 mol) and hydrazine hydrate 99% (0.5 g, 0.01 mol) in ethanol (30 mL) was heated under reflux for 14 h. The reaction mixture was cooled and the precipitated solid was collected by filtration, washed with water, dried and crystallized from ethanol.

5.1.16.2. Method B. A mixture of compound **20** (0.337 g, 0.001 mol) and hydrazine hydrate 99% (0.5 g, 0.01 mol) in ethanol (30 mL) was heated under reflux for 8 h. The reaction mixture was cooled and the precipitated solid was collected by filtration, washed with water, dried and crystallized from ethanol.

Yield 38% (method A); 51% (method B), m.p. 202–204 °C. IR (KBr, ν , cm^{-1}): 3233, 3115 (NH₂, NH), 1685 (C=O). ^1H NMR: (DMSO- d_6 , δ ppm): 4.15 (s, 2H, NH₂), 6.30–7.15 (m, 3H, Ar-H), 7.85 (s, 1H, pyrimidine-H), 12.55 (s, 1H, NH). ^{13}C NMR: (DMSO- d_6 , δ ppm): 102.4, 114.0, 117.1, 120.4, 124.9, 131.5, 144.7, 161.2, 164.7, 168.7 (Ar-C, triazole C-3), 176.3 (C=O), 185.9 (C=S). HRMS: m/z (ESI) calcd. for $\text{C}_{12}\text{H}_6\text{ClN}_6\text{O}_2\text{S}_2$, $[\text{M}-\text{H}]^-$: 348.9811; found: 348.9818.

5.1.17. 2-(8-Chloro-2-oxo-2H-pyrimido[2,1-b]benzothiazole-4-carbonyl)-N-(phenyl)hydrazine-1-carbothioamide (22)

A mixture of compound **12** (0.295 g, 0.001 mol) and phenyl isothiocyanate (0.135 g, 0.001 mol) in ethanol (15 mL) was heated under reflux for 10 h. The precipitated yellowish white solid was collected by filtration, washed with water, dried and crystallized from ethanol.

Yield 54%, m.p. 206–208 °C. IR (KBr, ν , cm^{-1}): 3330, 3210, 3115 (3NH), 1695, 1670 (2C=O). ^1H NMR: (DMSO- d_6 , δ ppm): 6.20–7.40 (m, 9H, Ar-H, pyrimidine-H), 10.20 (s, 1H, NH), 11.78 (s, 1H, NH), 13.63 (s, 1H, NH). ^{13}C NMR: (DMSO- d_6 , δ ppm): 110.2, 118.4, 123.5, 124.1, 124.9, 125.0, 128.9, 129.5, 138.3, 139.9, 161.0 (Ar-C), 163.7 (C=O), 174.3 (C=O), 187.7 (C=S). HRMS: m/z (ESI) calcd. for $\text{C}_{18}\text{H}_{11}\text{ClN}_5\text{O}_2\text{S}_2$, $[\text{M}-\text{H}]^-$: 428.0121; found: 428.0129. Anal. calcd. for $\text{C}_{18}\text{H}_{12}\text{ClN}_5\text{O}_2\text{S}_2$ (429.90): C, 50.29; H, 2.81; N, 16.29%. Found: C, 50.52; H, 2.73; N, 16.12%.

5.1.18. 8-Chloro-4-(5-(phenylamino)-[1,3,4]oxadiazol-2-yl)-2H-pyrimido[2,1-b]benzothiazol-2-one (23)

A mixture of compound **22** (0.43 g, 0.001 mol) and pyridine (5 mL) was heated under reflux for 6 h. The mixture was poured onto ice-water and the precipitated dark yellow solid was collected by filtration, washed with water, dried and crystallized from ethanol.

Yield 56%, m.p. 178–179 °C. IR (KBr, ν , cm^{-1}): 3110 (NH), 1690 (C=O). ^1H NMR: (DMSO- d_6 , δ ppm): 6.50–7.45 (m, 8H, Ar-H), 8.75 (s, 1H, pyrimidine-H), 10.65 (s, 1H, NH). ^{13}C NMR: (DMSO- d_6 , δ ppm): 118.4, 118.6, 120.6, 121.2, 124.1, 128.9, 129.1, 129.5, 132.0, 140.2, 140.8, 162.7, 167.5 (Ar-C), 181.5 (C=O). HRMS: m/z (ESI) calcd. for $\text{C}_{18}\text{H}_9\text{ClN}_5\text{O}_2\text{S}^-$, $[\text{M}-\text{H}]^-$: 394.0244; found: 394.0251. Anal. calcd. for $\text{C}_{18}\text{H}_{10}\text{ClN}_5\text{O}_2\text{S}$ (395.82): C, 54.62; H, 2.55; N, 17.69%. Found: C, 54.41; H, 2.72; N, 17.86%.

5.1.19. 8-Chloro-4-(5-(phenylamino)-[1,3,4]thiadiazol-2-yl)-2H-pyrimido[2,1-b]benzothiazol-2-one (24)

A mixture of compound **22** (0.43 g, 0.001 mol) and concentrated sulfuric acid (5 mL) was stirred at room temperature for 8 h. The mixture was poured onto ice-water and the precipitated dark yellow solid was collected by filtration, washed with water, dried and crystallized from ethanol.

Yield 54%, m.p. 193–195 °C. IR (KBr, ν , cm^{-1}): 3250 (NH), 1710 (C=O). ^1H NMR: (DMSO- d_6 , δ ppm): 6.45–7.78 (m, 8H, Ar-H), 8.65 (s, 1H, pyrimidine-H), 11.05 (s, 1H, NH). ^{13}C NMR: (DMSO- d_6 , δ ppm): 108.7, 118.0, 121.9, 122.1, 123.5, 125.1, 128.8, 129.1, 129.4, 139.1, 141.9, 143.2, 151.5, 161.8, 165.2 (Ar-C), 174.5 (C=O). HRMS: m/z (ESI) calcd for $\text{C}_{18}\text{H}_9\text{ClN}_5\text{O}_2\text{S}_2^-$, $[\text{M}-\text{H}]^-$: 410.0015; found: 410.0023.

5.2. Biological screening

5.2.1. Preliminary *in vitro* antitumor screening

Nineteen derivatives, **4–10** and **13–24** were selected by the National Cancer Institute (NCI) *in vitro* disease-oriented human cells screening panel assay to be evaluated for their *in vitro* antitumor activity. Preliminary *in vitro* single dose antitumor assay was performed using the full NCI-60 cell lines in accordance with the current protocol of the Drug Evaluation Branch, NCI, Bethesda [49–51]. These cell lines were incubated with a single concentration (10 μM) of each of the tested compounds. A 48 h continuous drug exposure protocol was used, and sulforhodamine B (SRB) assay was employed to estimate cell viability or growth. The data reported as mean-graph of the percentage growth of the treated cells, and presented as percentage growth inhibition (GI%) (Tables 1 and 2).

5.2.2. NCI full *in vitro* five dose antitumor assay

The human tumor cell lines of the cancer screening panel were grown in Roswell Park Memorial Institute (RPMI) 1640 medium containing 5% fetal bovine serum and 2 mM L-glutamine. For a typical screening experiment, cells were inoculated into multiwell microtiter plates at plating densities ranging from 5000 to 40,000 cells/well depending on the doubling time of individual cell lines. After cell inoculation, the microtiter plates were incubated at 37 °C, 5% CO₂, 95% air and 100% relative humidity for 24 h and then two plates of each cell line were fixed *in situ* with trichloroacetic acid (TCA) to represent a measurement of the cell population for each cell line at the time of compound addition. The tested compounds were solubilized in DMSO at 400-fold the desired final maximum test concentration and stored frozen prior to use. At the time of compound addition, an aliquot of frozen concentrate was thawed and diluted to twice the desired final maximum test concentration with complete medium containing 50 mg/mL gentamicin. Additional 4-, 10-fold or 1/2 log serial dilutions were made to

provide a total of five compound concentrations plus control. Aliquots of 100 mL of these dilutions were added to the appropriate microtiter wells already containing 100 mL of the medium, resulting in the required final compound concentrations. Following compound addition, the plates were incubated for additional 48 h at 37 °C, 5% CO₂, 95% air, and 100% relative humidity. For adherent cells, the assay was terminated by the addition of cold TCA. Cells were fixed *in situ* by gentle addition of 50 mL of cold 50% (w/v) TCA (final concentration, 10% TCA) and incubated for 1 h at 4 °C. The supernatant was discarded, and the plates were washed five times with tap water and air dried. Sulforhodamine B (SRB) solution (100 mL) at 0.4% (w/v) in 1% acetic acid was added to each well, and the plates were incubated for 10 min at room temperature. After staining, unbound dye was removed by washing five times with 1% acetic acid and the plates were air dried. Bound stain was subsequently solubilized with 10 mM trizma base and the absorbance was read on an automated plate reader at a wavelength of 515 nm. For suspension cells, the methodology was the same except that the assay was terminated by fixing settled cells at the bottom of the wells by gently adding 50 mL of 80% TCA (final concentration, 16% TCA) [49–51]. GI₅₀ values (μM) of the tested compounds over the most sensitive cell line of each tumor subpanel are listed in Table 3. The mean of the three response parameters (GI₅₀, TGI, and LC₅₀) over *in vitro* subpanel cancer cell lines are listed in Tables 4 and 5.

5.3. 3D pharmacophore elucidation

The 2D structures of the compounds were built and then converted into the 3D with the help of vLife MDS 3.0 software. The 3D structures were then energetically minimized up to the rms gradient of 0.01 using the CHARMM22 force field. All conformers were then energetically minimized up to the rms gradient of 0.01 and then saved in separate folder. LigandScout software [53] was used to generate 3D pharmacophore maps for structural features of the compounds. For each ligand, the most plausible conformation was selected based on its ability to fulfill the essential chemical features described in the 3D pharmacophore.

Acknowledgments

The authors would like to express their sincere thanks to the staff members of the Department of Health and Human Services, National Cancer Institute (NCI), Bethesda, Maryland, USA, for performing the antitumor screening of the newly synthesized compounds. Thanks also to Georgia State University, USA, for carrying out the spectral and elemental analyses.

Appendix A. Supplementary data

Supplementary data related to this article can be found at <http://dx.doi.org/10.1016/j.ejmech.2014.07.097>.

References

- [1] A. Jemal, R. Siegel, E. Ward, T. Murray, J. Xu, M.J. Thun, Cancer statistics, *CA Cancer J. Clin.* 57 (2007) 43–66.
- [2] P. Anand, A.B. Kunnumakara, C. Sundaram, K.B. Harikumar, S.T. Tharakan, O.S. Lai, B. Sung, B.B. Aggarwal, Cancer is a preventable disease that requires major lifestyle changes, *Pharm. Res.* 25 (2008) 2097–2116.
- [3] L.V. Peng-Cheng, C.F. Zhou, J. Chen, P.G. Liu, K.R. Wang, W.J. Mao, L. Huan-Qiu, Y. Yang, J. Xiong, H.L. Zhu, Design, synthesis and biological evaluation of thiazolidinone derivatives as potential EGFR and HER-2 inhibitors, *Bioorg. Med. Chem.* 18 (2010) 314–319.
- [4] M. Reck, N.V. Zandwijk, C. Gridelli, Z. Baliko, D. Rischin, S. Allan, M. Krzakowski, D. Heigener, Erlotinib in advanced non-small cell lung cancer: efficacy and safety findings of the global phase IV Tarceva lung cancer survival treatment study, *J. Thorac. Oncol.* 5 (2010) 1616–1622.
- [5] J. Smith, Erlotinib: small-molecule targeted therapy in the treatment of non small-cell lung cancer, *Clin. Ther.* 27 (2005) 1513–1534.
- [6] K. Tamura, M. Fukuoka, Gefitinib in non-small cell lung cancer, *Expert. Opin. Pharmacother.* 6 (2005) 985–993.
- [7] M.T. Gabr, N.S. El-Gohary, E.R. El-Bendary, M.M. El-Kerdawy, New series of benzothiazole and pyrimido[2,1-*b*]benzothiazole derivatives: synthesis, antitumor activity, EGFR tyrosine kinase inhibitory activity and molecular modeling studies, *Med. Chem. Res.* (29 July 2014), <http://dx.doi.org/10.1007/s00044-014-1114-x>. Published online.
- [8] X.-H. Shi, Z. Wang, Y. Xia, T.-H. Ye, M. Deng, Y.-Z. Xu, Y.-Q. Wei, L.-T. Yu, Synthesis and biological evaluation of novel benzothiazole-2-thiol derivatives as potential anticancer agents, *Molecules* 17 (2012) 3933–3944.
- [9] H.S. Elzahabi, Synthesis, characterization of some benzazoles bearing pyridine moiety: search for novel anticancer agents, *Eur. J. Med. Chem.* 46 (2011) 4025–4034.
- [10] S. Saeed, N. Rashid, P.G. Jones, M. Ali, R. Hussain, Synthesis, characterization and biological evaluation of some thiourea derivatives bearing benzothiazole moiety as potential antimicrobial and anticancer agents, *Eur. J. Med. Chem.* 45 (2010) 1323–1331.
- [11] W.P. Hu, Y.K. Chen, C.C. Liao, H.S. Yu, Y.M. Tsai, S.M. Huang, F.Y. Tsai, H.C. Shen, L.S. Chang, J.J. Wang, Synthesis, and biological evaluation of 2-(4-aminophenyl)benzothiazole derivatives as photosensitizing agents, *Bioorg. Med. Chem.* 18 (2010) 6197–6207.
- [12] Y.A. Al-Soud, H.H. Al-Sa'doni, B. Saeed, I.H. Jaber, M.O. Beni-Khalid, N.A. Al-Masoudi, T. Abdul-Kadir, P. La Colla, B. Busonera, T. Sanna, R. Loddio, Synthesis and *in vitro* antiproliferative activity of new benzothiazole derivatives, *ARKIVOC xv* (2008) 225–238.
- [13] C.G. Mortimer, G. Wells, J.P. Crochard, E.L. Stone, T.D. Bradshaw, M.F.G. Stevens, A.D. Westwell, Antitumor benzothiazoles. 26. 2-(3,4-dimethoxyphenyl)-5-fluorobenzothiazole (GW 610, NSC 721648), a simple fluorinated 2-arylbenzothiazole, shows potent and selective inhibitory activity against lung, colon and breast cancer cell lines, *J. Med. Chem.* 49 (2006) 179–185.
- [14] E. Brantley, S. Antony, G. Kohlhagen, L.H. Meng, K. Agama, S.F. Stinson, E.A. Sausville, Y. Pommier, Anti-tumor drug candidate 2-(4-amino-3-methylphenyl)-5-fluorobenzothiazole induces single-strand breaks and DNA-protein cross-links in sensitive MCF-7 breast cancer cells, *Cancer Chemother. Pharmacol.* 58 (2006) 62–72.
- [15] C.J. Lion, C.S. Matthews, G. Wells, T.D. Bradshaw, M.F.G. Stevens, A.D. Westwell, Antitumor properties of fluorinated benzothiazole-substituted hydroxycyclohexa-2,5-dienones ('quinols'), *Bioorg. Med. Chem. Lett.* 16 (2006) 5005–5008.
- [16] S.T. Huang, I.J. Hsei, C. Chen, Synthesis and anticancer evaluation of bis(benzimidazoles), bis(benzoxazoles), and benzothiazoles, *Bioorg. Med. Chem.* 14 (2006) 6106–6119.
- [17] E. Kashiyama, I. Hutchinson, M.S. Chua, S.F. Stinson, L.R. Phillips, G. Kaur, E.A. Sausville, T.D. Bradshaw, A.D. Westwell, M.F.G. Stevens, Antitumor benzothiazoles. 8. Synthesis, metabolic formation, and biological properties of the C- and N-oxidation products of antitumor 2-(4-aminophenyl)benzothiazoles, *J. Med. Chem.* 42 (1999) 4172–4184.
- [18] T.D. Bradshaw, S. Wrigley, D.F. Shi, R.J. Schultz, K.D. Paull, M.F.G. Stevens, 2-(4-Aminophenyl)benzothiazoles: novel agents with selective profiles of *in vitro* anti-tumour activity, *Br. J. Cancer* 77 (1998) 745–752.
- [19] N. Karali, O. Güzel, N. Ozsoy, S. Ozbey, A. Salman, Synthesis of new spiroindolinones incorporating a benzothiazole moiety as antioxidant agents, *Eur. J. Med. Chem.* 45 (2010) 1068–1077.
- [20] D. Cressier, C. Prouillac, P. Hernandez, C. Amourette, M. Diserbo, C. Lion, G. Rima, Synthesis, antioxidant properties and radioprotective effects of new benzothiazoles and thiadiazoles, *Bioorg. Med. Chem.* 17 (2009) 5275–5284.
- [21] V.K. Deshmukh, P. Raviprasad, P.A. Kulkarni, S.V. Kuberkar, Design, synthesis and biological activities of novel 4*H*-pyrimido[2,1-*b*][1,3]benzothiazole derivatives, *Int. J. ChemTech Res.* 3 (2011) 136–142.
- [22] M.S. Chaitanya, G. Nagendrappa, V.P. Vaidya, Synthesis, biological and pharmacological activities of 2-methyl-4*H*-pyrimido[2,1-*b*][1,3]benzothiazoles, *J. Chem. Pharm. Res.* 2 (2010) 206–213.
- [23] S. Gupta, N. Ajmera, N. Gautam, R. Sharma, D.C. Gautam, Novel synthesis and biological activity study of pyrimido[2,1-*b*]benzothiazoles, *Indian J. Chem.* 48B (2009) 853–858.
- [24] M.A. El-Sherbeny, Synthesis of certain pyrimido[2,1-*b*]benzothiazole and benzothiazolo[2,3-*b*]quinazoline derivatives for *in vitro* antitumor and antiviral activities, *Arzneim. Forsch.* 50 (2000) 848–853.
- [25] P.R. Prasad, S.D. Shinde, G.S. Waghmare, V.L. Naik, K. Bhuvaneshwari, S.V. Kuberkar, Synthesis and *in vitro* anticancer activity of 9-chloro-3-cyano-8-fluoro-2-methylthio-4-oxo-4*H*-pyrimido[2,1-*b*][1,3]benzothiazole and its 2-substituted derivatives, *J. Chem. Pharm. Res.* 3 (2011) 20–27.
- [26] L.B. Labhsetwar, R.G. Shendarkar, S.V. Kuberkar, Synthesis and *in vitro* anticancer activity of 8-chloro-3-cyano-4-imino-2-methylthio-4*H*-pyrimido[2,1-*b*][1,3]benzothiazole and its 2-substituted derivatives, *Asian J. Pharm. Res. Health Care* 2 (2010) 273–278.
- [27] F. Manetti, C. Brullo, M. Magnani, F. Mosci, B. Chelli, E. Crespan, S. Schenone, A. Naldini, O. Bruno, M.L. Trincavelli, G. Maga, F. Carraro, C. Martini, F. Bondavalli, M. Botta, Structure-based optimization of pyrazolo[3,4-*d*]pyrimidines as Abl inhibitors and antiproliferative agents toward human leukemia cell lines, *J. Med. Chem.* 51 (2008) 1252–1259.

- [28] D. Menche, J. Hassfeld, F. Sasse, M. Huss, H. Wiczorek, Design, synthesis, and biological evaluation of novel analogues of archazolid: a highly potent simplified V-ATPase inhibitor, *Bioorg. Med. Chem.* 15 (2007) 1732–1735.
- [29] G. Daidone, B. Maggio, D. Raffa, S. Plescia, D. Schillaci, M.V. Raimondi, Synthesis and *in vitro* antileukemic activity of new 4-triazenopyrazole derivatives, *Il Farmaco* 59 (2004) 413–417.
- [30] S. Hanan, R. El Mostapha, A.A. Medaghri, H. Abderrafia, A. El Malki, Synthesis and *in vitro* cytotoxic activity of novel pyrazole-3,4-dicarboxylates, *Int. J. Org. Chem.* 3 (2013) 37–41.
- [31] A.R. Farghaly, Synthesis of some new indole derivatives containing pyrazoles with potential antitumor activity, *ARKIVOC xi* (2010) 177–187.
- [32] A.M. Farag, A.S. Mayhoub, S.E. Barakat, A.H. Bayomi, Regioselective synthesis and antitumor screening of some novel N-phenylpyrazole derivatives, *Bioorg. Med. Chem.* 16 (2008) 881–889.
- [33] Y. Xia, C.D. Fan, B.X. Zhao, J. Zhao, D.S. Shin, J.Y. Miao, Synthesis and structure-activity relationships of novel 1-arylmethyl-3-aryl-1H-pyrazole-5-carbohydrazide hydrazone derivatives as potential agents against A549 lung cancer cells, *Eur. J. Med. Chem.* 43 (2008) 2347–2353.
- [34] Y. Xia, Z.W. Dong, B.X. Zhao, X. Ge, N. Meng, D.S. Shin, J.Y. Miao, Synthesis and structure-activity relationships of novel 1-arylmethyl-3-aryl-1H-pyrazole-5-carbohydrazide derivatives as potential agents against A549 lung cancer cells, *Bioorg. Med. Chem.* 15 (2007) 6893–6899.
- [35] A. Balbi, M. Anzaldi, C. Maccio, C. Aiello, M. Mazzei, R. Gangemi, P. Castagnola, M. Miele, C. Rosano, M. Viale, Synthesis and biological evaluation of novel pyrazole derivatives with anticancer activity, *Eur. J. Med. Chem.* 46 (2011) 5293–5309.
- [36] S. Bindi, D. Fancelli, C. Alli, D. Berta, J.A. Bertrand, A.D. Cameron, P. Cappella, P. Carpinelli, G. Cervi, V. Croci, M. D'Anello, B. Forte, M.L. Giorgini, A. Marsiglio, J. Moll, E. Pesenti, V. Pittalà, M. Pulici, F. Riccardi-Sirtori, F. Roletto, C. Soncini, P. Storici, M. Varasi, D. Volpi, P. Zugnoni, P. Vianello, Thieno[3,2-c]pyrazoles: a novel class of Aurora inhibitors with favorable antitumor activity, *Bioorg. Med. Chem.* 18 (2010) 7113–7120.
- [37] P. Pevarello, D. Fancelli, A. Vulpetti, R. Amici, M. Villa, V. Pittalà, P. Vianello, A. Cameron, M. Ciomei, C. Mercurio, J.R. Bischoff, F. Roletto, M. Varasi, M.G. Brasca, 3-Amino-1,4,5,6-tetrahydropyrrrolo[3,4-c]pyrazoles: a new class of CDK2 inhibitors, *Bioorg. Med. Chem. Lett.* 16 (2006) 1084–1090.
- [38] D. Fancelli, D. Berta, S. Bindi, A. Cameron, P. Cappella, P. Carpinelli, C. Catana, B. Forte, P. Giordano, M.L. Giorgini, S. Mantegani, A. Marsiglio, M. Meroni, J. Moll, V. Pittalà, F. Roletto, D. Severino, C. Soncini, P. Storici, R. Tonani, M. Varasi, A. Vulpetti, P. Vianello, Potent and selective Aurora inhibitors identified by the expansion of a novel scaffold for protein kinase inhibition, *J. Med. Chem.* 48 (2005) 3080–3084.
- [39] M.A.Z. Abu-Zaied, G.A.M. Nawwar, R.H. Swellem, S.H. El-Sayed, Synthesis and screening of new 5-substituted-1,3,4-oxadiazole-2-thioglycosides as potent anticancer agents, *Pharmacology & Pharmacy* 3 (2012) 254–261.
- [40] V.K.R. Sahu, A.K. Singh, D. Yadav, Review article on 1,3,4-oxadiazole derivatives and its pharmacological activities, *Int. J. ChemTech. Res.* 3 (2011) 1362–1372.
- [41] S.K. Jain, A.K. Yadav, P. Nayak, 3D QSAR Analysis on oxadiazole derivatives as anticancer agents, *Int. J. Pharm. Sci. Drug. Res.* 3 (2011) 230–235.
- [42] X. Ouyang, E.L. Piatnitski, V. Pattaropong, X. Chen, H.-Y. He, A.S. Kiselyov, A. Velankar, J. Kawakami, M. Labelle, L. Smith II, J. Lohman, S.P. Lee, A. Malikzay, J. Fleming, J. Gerlak, Y. Wang, R.L. Rosler, K. Zhou, S. Mitelman, M. Camara, D. Surguladze, J.F. Doody, M.C. Tuma, Oxadiazole derivatives as a novel class of antimetabolic agents: synthesis, inhibition of tubulin polymerization, and activity in tumor cell lines, *Bioorg. Med. Chem. Lett.* 16 (2006) 1191–1196.
- [43] B. Peter, H.B. Robert, S.H. Craig, F.A.H. Laurent, H. Mark, G.K. Jason, K. Jane, K. Teresa, J.O. Donald, E.P. Stuart, J.W. Emma, W. Ingrid, Inhibitors of epidermal growth factor receptor tyrosine kinase: optimisation of potency and *in vivo* pharmacokinetics, *Bioorg. Med. Chem. Lett.* 16 (2006) 4908–4912.
- [44] M. Ranson, Epidermal growth factor receptor tyrosine kinase inhibitors, *Br. J. Cancer* 90 (2004) 2250–2255.
- [45] M.N. Noolvi, H.M. Patel, M. Kaur, Benzothiazoles: search for anticancer agents, *Eur. J. Med. Chem.* 54 (2012) 447–462.
- [46] D. Fabbro, S. Ruetz, E. Buchdunger, S.W. Cowan-Jacob, G. Fendrich, J. Liebetanz, T. O'Reilly, P. Traxler, B. Chaudhari, H. Fretz, J. Zimmermann, T. Meyer, G. Carvatti, P. Furet, P.W. Manley, Protein kinases as targets for anticancer agents: from inhibitors to useful drugs, *Pharmacol. Ther.* 93 (2002) 79–98.
- [47] M.T. Gabr, N.S. El-Gohary, E.R. El-Bendary, M.M. El-Kerdawy, EGFR tyrosine kinase targeted compounds: *in vitro* antitumor activity and molecular modeling studies of new benzothiazole and pyrimido[2,1-*b*]benzothiazole derivatives, *ECXL* 13 (2014) 573–585.
- [48] M.T. Gabr, N.S. El-Gohary, E.R. El-Bendary, M.M. El-Kerdawy, Structure-based drug design and biological evaluation of 2-acetamidobenzothiazole derivative as EGFR kinase inhibitor, *J. Enzyme Inhib. Med. Chem.* (5 March 2014), <http://dx.doi.org/10.3109/14756366.2014.887707>. Published online.
- [49] M.R. Grever, S.A. Schepartz, B.A. Chabner, The National Cancer Institute: cancer drug discovery and development program, *Semin. Oncol.* 19 (1992) 622–638.
- [50] M.R. Boyd, K.D. Paull, Some practical considerations and applications of the National Cancer Institute *in vitro* anticancer drug discovery screen, *Drug. Rev.* 34 (1995) 91–109.
- [51] A. Monks, D. Scudiero, P. Skehan, R. Shoemaker, K. Paull, D. Vistica, C. Hose, J. Jangley, P. Cronis, A. Viagro-Wolff, M. Gray-Goodrich, H. Campell, M. Boyd, Feasibility of a high-flux anticancer drug screen using a diverse panel of cultured human tumor cell lines, *J. Natl. Cancer Inst.* 83 (1991) 757–766.
- [52] J.S. Mason, A.C. Good, E.J. Martin, 3-D pharmacophores in drug discovery, *Curr. Pharm. Des.* 7 (2001) 567–597.
- [53] G. Wolber, T. Langer, LigandScout: 3D Pharmacophores derived from protein-bound ligands and their use as virtual screening filters, *J. Chem. Inf. Comput. Sci.* 45 (2005) 160–169.